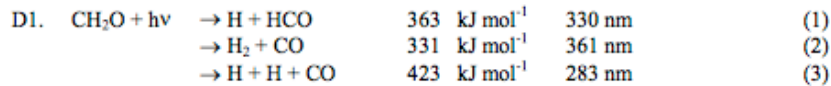


Comparison of GEOS-Chem Photolysis Rates

D1 – CH2O



Applies to: CH2O

The recommended quantum yields are listed in Table 4D-4 and are based on a polynomial fit over the wavelength range 250 – 338 nm of the data for $\Phi_1(\text{H} + \text{HCO})$ from Lewis et al. [104], Marling [119], Horowitz and Calvert [84], Clark et al. [47], Tang et al. [188], Moortgat et al. [139], Smith et al. [179], Pope et al. [159, 160], and Gorroategi Carbajo et al. [74].

$$\Phi_1(\text{H} + \text{HCO}) = a_0 + a_1\lambda + a_2\lambda^2 + a_3\lambda^3 + a_4\lambda^4$$

where

$$a_0 = 557.95835182$$

$$a_1 = -7.31994058026$$

$$a_2 = 0.03553521598$$

$$a_3 = -7.54849718 \times 10^{-5}$$

$$a_4 = 5.91001021 \times 10^{-8}$$

$\Phi_2(\text{H}_2 + \text{CO})$ was optimized using the quantum data for CO from Moortgat et al. [139] and the relation $\Phi_2(\text{H}_2 + \text{CO}) = \Phi_{\text{tot}} - \Phi_1(\text{H} + \text{HCO})$. The pressure and temperature dependence of $\Phi_2(\text{H}_2 + \text{CO})$ is based on the algorithm cited in Calvert et al. [33] and is limited to wavelengths > 330 nm. The pressure dependence of $\Phi_2(\text{H}_2 + \text{CO})$ is represented in Stern-Volmer form

$$\Phi_2(\text{H}_2 + \text{CO}) = \left[\frac{1}{\frac{1}{(1 - \Phi_1(\lambda))} + \alpha(\lambda, T) \times P} \right]^{-1}$$

where $\alpha(\lambda, T)$ is the quenching coefficient whose values at 300 K can be estimated directly from Φ_1 and Φ_2

$$\alpha(\lambda, 300 \text{ K}) = \left[\frac{1}{\Phi_2(\lambda, 300 \text{ K})} - \frac{1}{(1 - \Phi_1(\lambda))} \right]^{-1}$$

where the quantum yields at standard pressure (1 atmosphere) and 300 K are given in Table 4D-4.

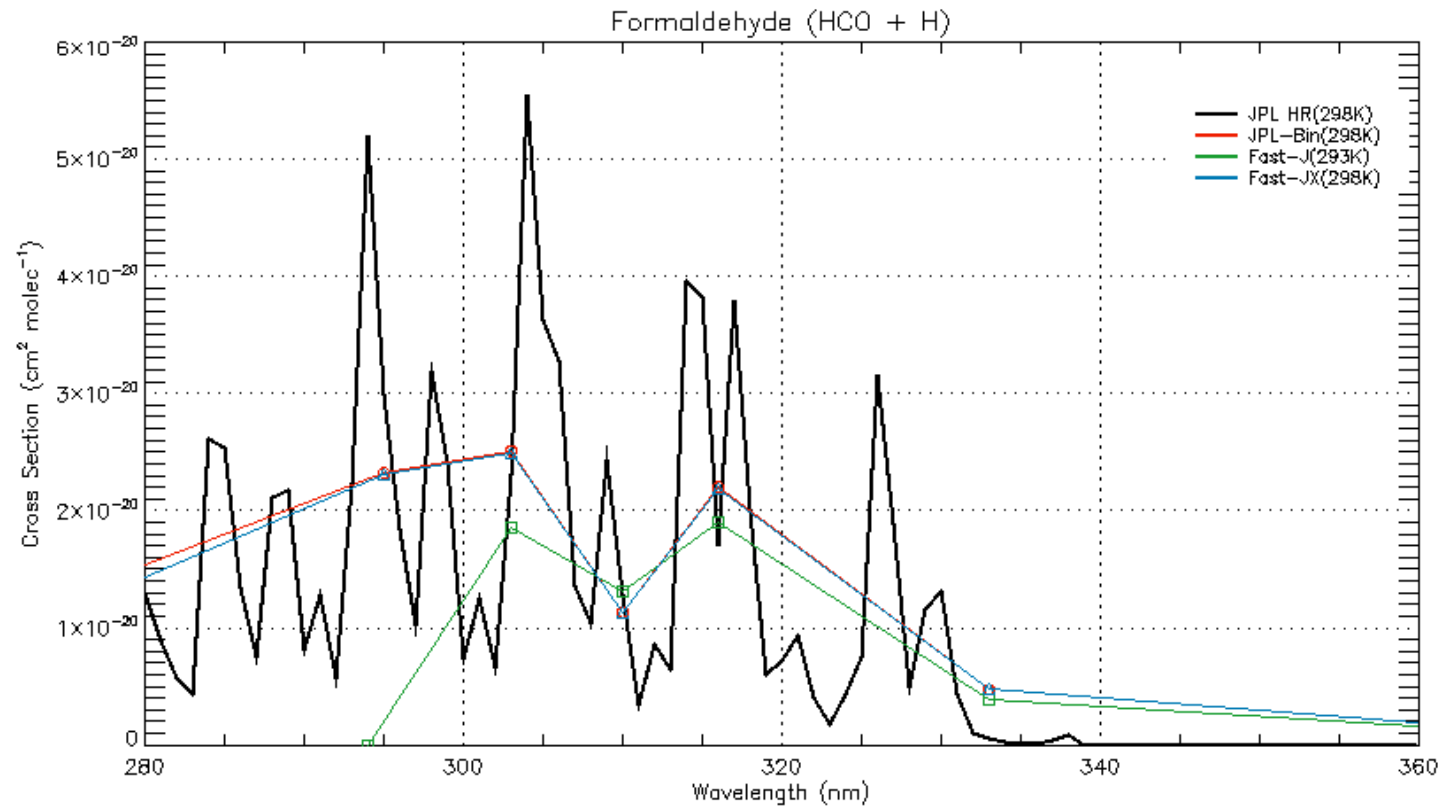
At temperatures between 220 and 300 K the quenching coefficient $\alpha(\lambda, T)$ can be calculated using

4D-3

$$\alpha(\lambda, T) = \alpha(\lambda, 300 \text{ K}) \times \left\{ 1 + 0.05 \times (\lambda - 329) \times \left[\frac{(300 - T)}{80} \right] \right\}$$

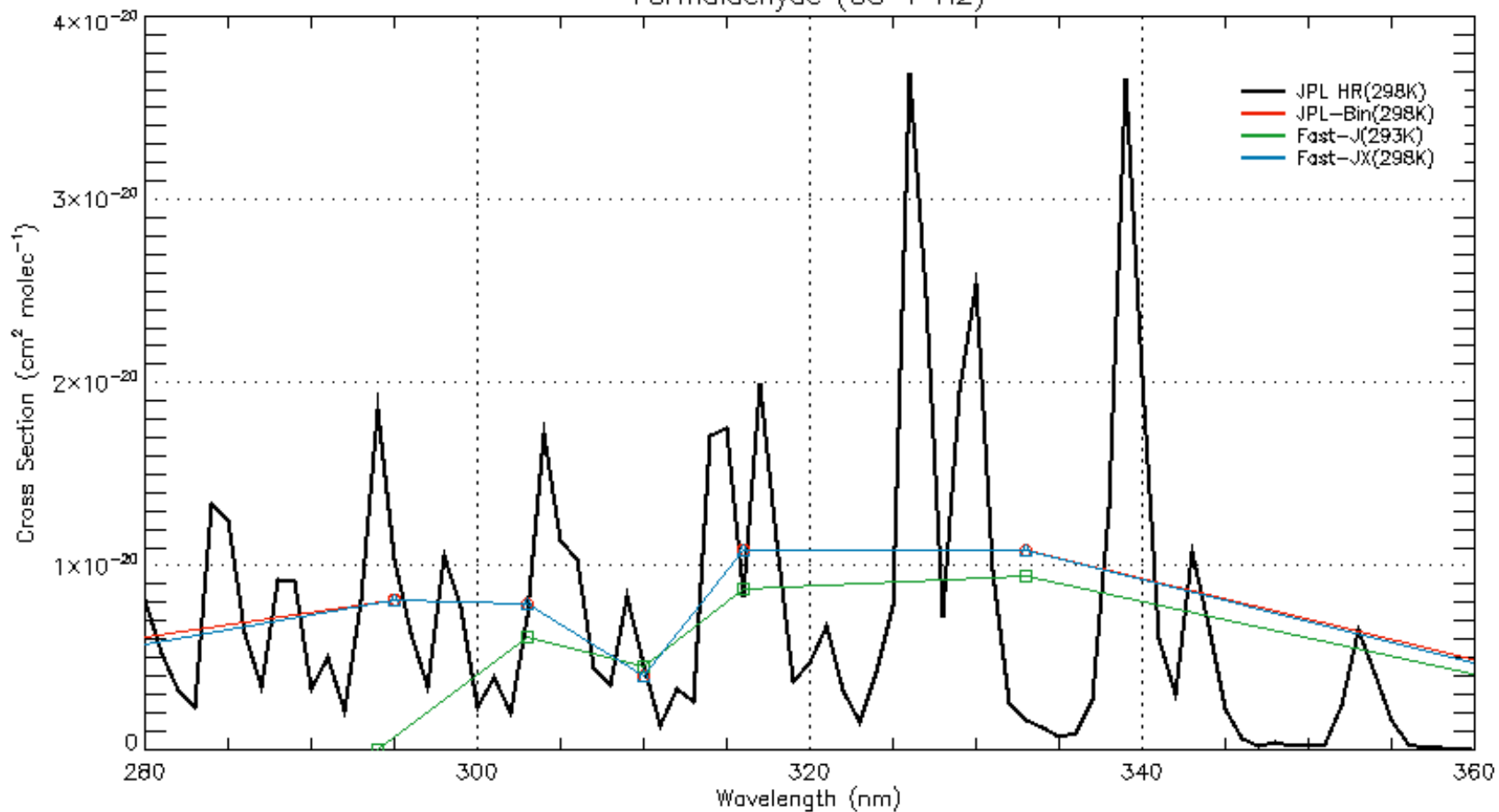
The formulae given above for the pressure and temperature dependence of the quantum yields are recommended.

Channel 1 (H+HCO)

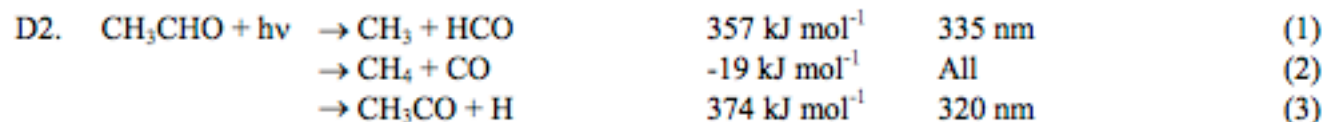


Channel 2 (H2+CO)

Formaldehyde (CO + H2)



D2 – ALD2



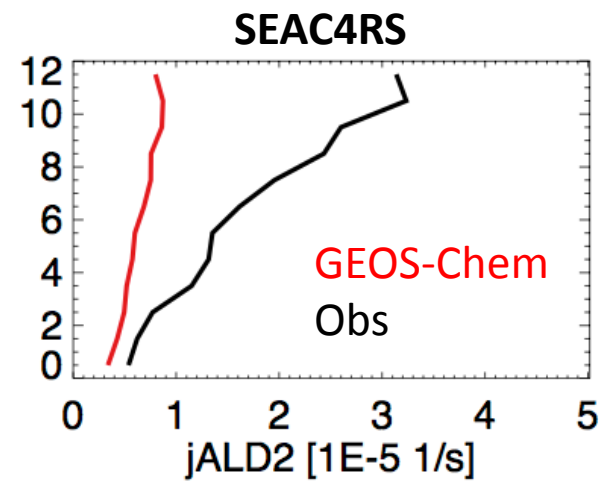
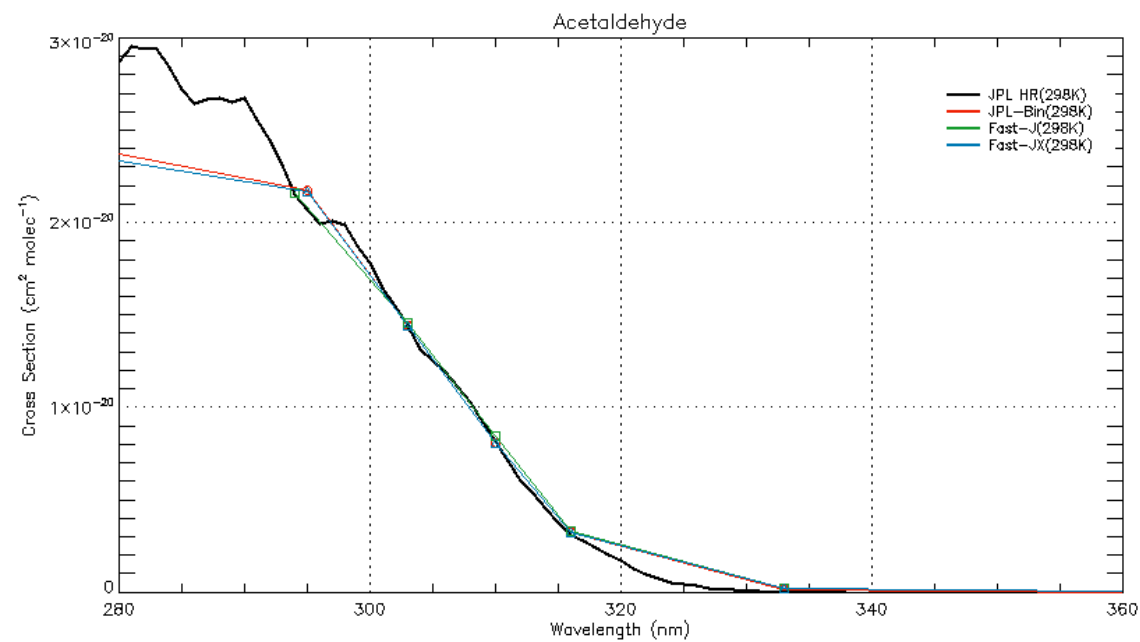
(Recommendation: 06-2, Note: 10-6, Evaluated: 10-6)

Photolysis Quantum Yield and Product Studies: The photodissociation quantum yield of CH_3CHO and the product quantum yields are wavelength and pressure dependent. Quantum yield measurements have been reported by Calvert and Pitts [36] and Weaver et al. [203] at isolated wavelengths between 290 and 332 nm. Quantum yields of CO , CH_4 and CO_2 were determined in the photolysis of trace concentrations of CH_3CHO in air and N_2 in the spectral range 250 – 330 nm at 1 atmospheric pressure by Meyrahn et al. [133], which allowed the determination of $(\Phi_1 + \Phi_2)$, Φ_2 , and Φ_3 . The product quantum yield pressure dependence was also investigated by Meyrahn [132] at 270, 303.4 and 313 nm. Horowitz et al. [86] and Horowitz and Calvert [85] measured the quantum yields of CO , CH_4 and H_2 formation at 290, 300, 313, 320 and 332 nm in the presence of various pressures of O_2 and CO_2 from which Φ_1 and Φ_2 were derived. There is evidence from the studies of Meyrahn et al. [132, 133] and Horowitz et al. [86] that some CO_2 is formed from secondary reactions of the CH_3CO radical that is produced in channel (3). The quantum yield for channel 3 was estimated to be 0.025 at 300 nm and to decrease to zero at 320 nm. Both Meyrahn et al. [132, 133] and Horowitz et al. [85, 86] observed a pressure dependence of the product yields, from which Stern-Volmer quenching coefficients were derived. These data were summarized by Calvert et al. [33].

The quantum yield recommendation given in Table 4D-6 for room temperature and atmospheric pressure are based on the evaluation by Atkinson and Lloyd [11] and the measurements by Horowitz and Calvert [85], Meyrahn et al. [133] and Meyrahn [132].

Applies to: ALD2

Channel 1+2



D3 – RCHO

D3.	$C_2H_3CHO + hv$	$\rightarrow C_2H_3 + HCO$	351 kJ mol^{-1}	341 nm	(1)
		$\rightarrow C_2H_6 + CO$	-8 kJ mol^{-1}	All	(2)
		$\rightarrow C_2H_4 + HCHO$	129 kJ mol^{-1}	926 nm	(3)
		$\rightarrow CH_3 + CH_2CHO$	343 kJ mol^{-1}	349 nm	(4)

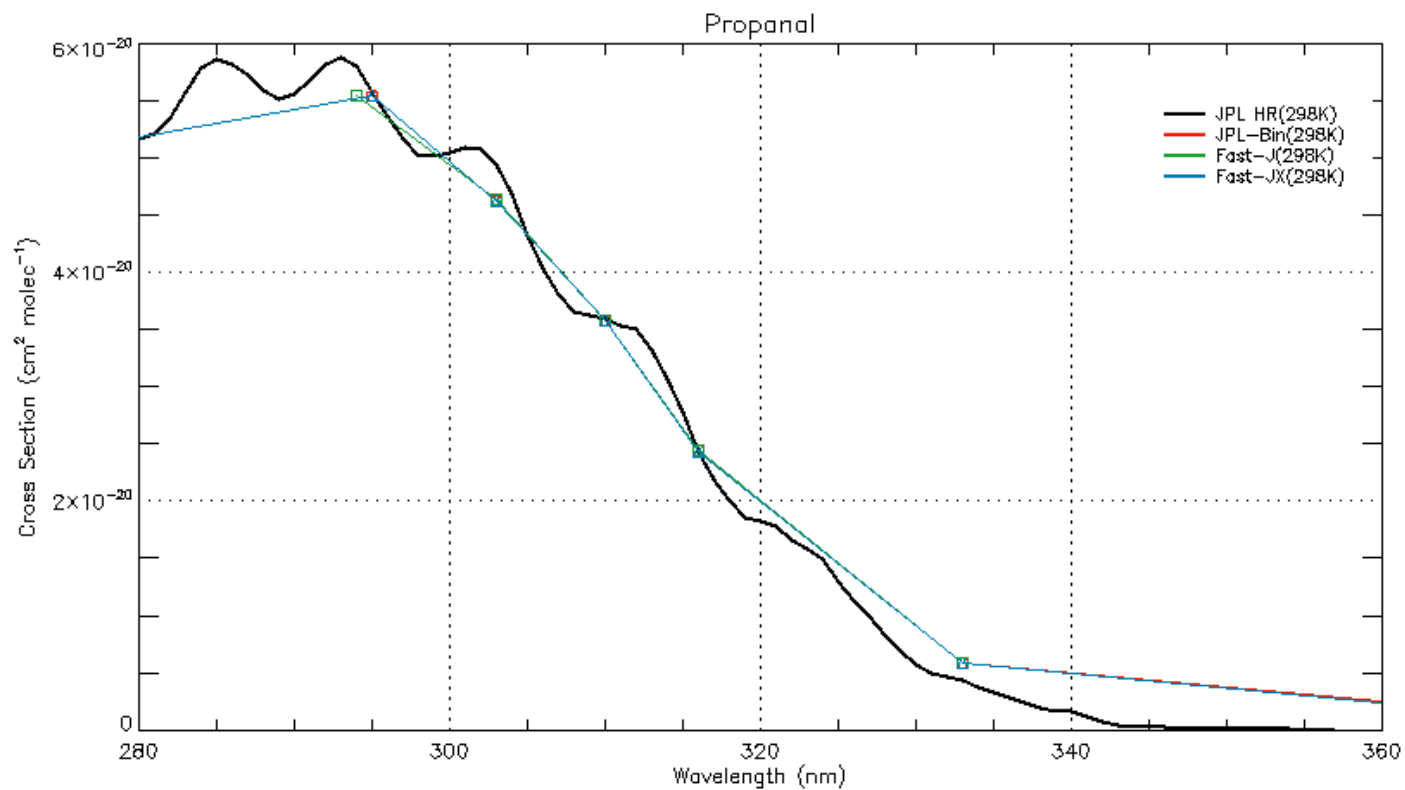
Photolysis Quantum Yield and Product Studies: Quantum yield measurements have been performed by Heicklen et al. [80] and Chen and Zhu [43]. Heicklen et al. [80] measured the quantum yield of HO_2 and $C_2H_3O_2$ radicals (in air bath gas) using laser photolysis at 294, 302, 312 and 325 nm combined with UV absorption to determine Φ_1 . Quantum yields of CO and C_2H_6 were obtained in steady-state photolysis (at 254, 312 and 334 nm) experiments in O_2 where $\Phi_1 = \Phi(CO) - \Phi(C_2H_6)$ and $\Phi_2 = \Phi(C_2H_6)$. A Stern-Volmer pressure dependence of the quantum yields was observed at all wavelengths, i.e., lower quantum yields at higher pressures. At atmospheric pressure, values of $\Phi_1 = 0.22, 0.89, 0.85, 0.50, 0.26$ and 0.15 were derived at 254, 294, 302, 313, 325 and 334 nm, respectively. Heicklen et al. [80] reported $\Phi_2 = 0.33$ for 254 nm photolysis and $\Phi_2 = 0$ at longer wavelengths. The contribution of other primary processes (Φ_3 and Φ_4) was found to increase at wavelengths <265 nm from earlier studies as cited in Calvert and Pitts [36].

Chen and Zhu [43] measured the quantum yield of HCO radicals (Φ_1) over the wavelength range 280 – 330 nm using time-resolved cavity ring-down spectroscopy with detection of HCO at 613.8 nm. The reported HCO yields are 0.85 ± 0.06 at 280 nm, 1.01 ± 0.07 at 285 nm, 0.95 ± 0.06 at 290 nm, 0.98 ± 0.06 at 295 nm, 0.92 ± 0.06 at 300 nm, 0.95 ± 0.08 at 305 nm, 0.98 ± 0.11 at 310 nm, 0.91 ± 0.05 at 315 nm, 1.08 ± 0.07 at 320 nm, 1.07 ± 0.14 at 325 nm, and 0.84 ± 0.08 at 330 nm. These values are quoted for zero-pressure but no pressure dependence to the HCO quantum yield at any wavelength was observed for pressures over the range 10 – 400 Torr N_2 .

The quantum yield studies by Heicklen et al. [80] and Chen and Zhu [43] are only in agreement in the narrow wavelength range 290 – 305 nm. At $\lambda > 305$ nm, the data of Chen and Zhu do not show the decrease of Φ_1 reported by Heicklen et al [80]. Because of the discrepancies between these data sets no quantum yield recommendation is given.

Applies to: RCHO

Channel 1



D9 – MP

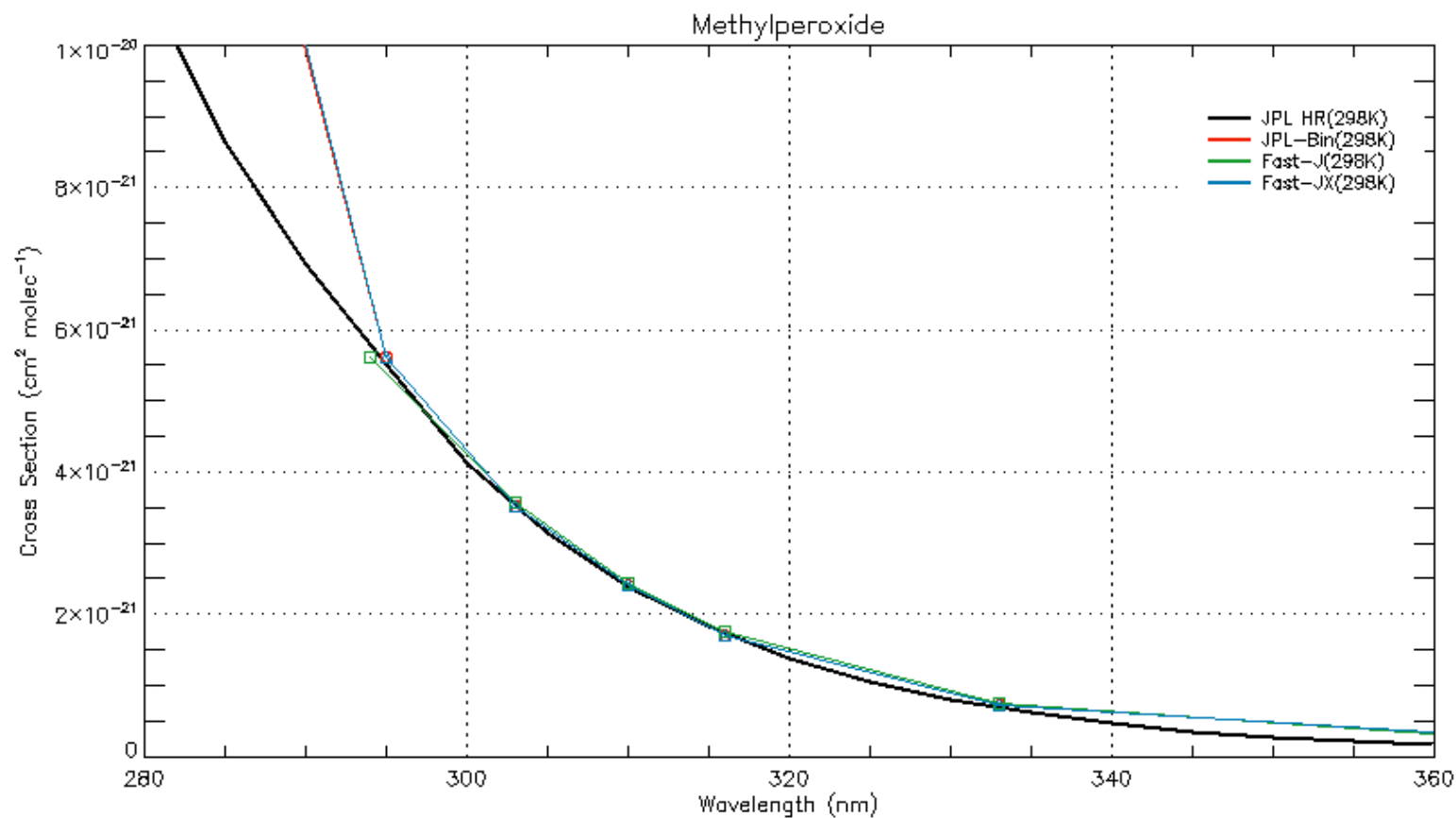


Photolysis Quantum Yields and Product Studies: CH_3OOH dissociates upon light absorption to give CH_3O with unit quantum yield, $\Phi_1 = 1.00 \pm 0.18$ (Vaghjiani and Ravishankara [194]). These authors also observed some production of H (quantum yield of 0.038 ± 0.007) and O atoms (quantum yield < 0.007) at shorter wavelengths (i.e., 193 nm).

Thelen et al. [190] report unit quantum yields for OH production at 248 and 193 nm that are in agreement with the results of Vaghjiani and Ravishankara [193]. Quantum yields for OH and CH_3O were also measured by Blitz et al. [22] in the wavelength range 223 – 355 nm. These authors have shown that the quantum yield for both OH and CH_3O production is unity across this range of wavelengths.

Applies to: MP, ETP, RA3P, RB3P, R4P, RP, MAP, INPN, PRPN, PP, RIP, IAP, ISNP, VRP, MRP, MAOP, ATOOH

Channel 1



D12 –R4N2

D12. $\text{CH}_3\text{ONO}_2 + h\nu \rightarrow \text{CH}_3\text{O} + \text{NO}_2$	172 kJ mol ⁻¹	697 nm	(1)
$\rightarrow \text{HCHO} + \text{HONO}$		All	(2)
$\rightarrow \text{HCHO} + \text{NO} + \text{OH}$	240 kJ mol ⁻¹	497 nm	(3)
$\rightarrow \text{CH}_3\text{ONO} + \text{O}(^3\text{P})$	306 kJ mol ⁻¹	391 nm	(4)
$\rightarrow \text{CH}_3 + \text{NO}_3$	348 kJ mol ⁻¹	344 nm	(5)
$\rightarrow \text{CH}_2\text{ONO}_2 + \text{H}$	407 kJ mol ⁻¹	294 nm	(6)
$\rightarrow \text{CH}_3\text{O} + \text{NO} + \text{O}(^3\text{P})$	479 kJ mol ⁻¹	250 nm	(7)
$\rightarrow \text{CH}_3\text{ONO} + \text{O}(^1\text{D})$	496 kJ mol ⁻¹	241 nm	(8)

Absorption Cross Sections: The UV absorption spectrum of methyl nitrate (CH_3ONO_2) displays a strong continuous band in the region (190 – 250 nm) and a weaker band in the range (250 – 345 nm). The spectrum was measured at room temperature by McMillan [38] (201 – 323 nm), Maria et al. [114] (235 – 305 nm), Taylor et al. [189] (190 – 330 nm), Roberts and Fajer [165] (270 – 330 nm), Libuda and Zabel [106] (235 – 345 nm) and over a range of temperatures by Rattigan et al. [164] (220 – 335 nm) over the range 233 – 294 K and Talukdar et al. [186] (236 – 334 nm) over the range 240 – 360 K. Good agreement exists at wavelengths <240 nm between the absorption cross sections measured by Taylor et al. [189] and Rattigan et al. [164]. In the wavelength range 240 – 340 nm there is good agreement between the measurements of Roberts and Fajer [165], Libuda and Zabel [106], Rattigan et al. [164] and Talukdar et al. [186]. The values of Taylor et al. [189] are consistently larger at $\lambda > 270$ nm. Between 235 and 280 nm the absorption cross sections measured by Talukdar et al. [186] are nearly independent of temperature but for $\lambda > 290$ nm the cross sections decrease with decreasing temperature. At 330 nm the cross sections decrease by almost a factor of two between 298 and 240 K. Talukdar et al. [186] parameterized the absorption cross section temperature dependence using the expression

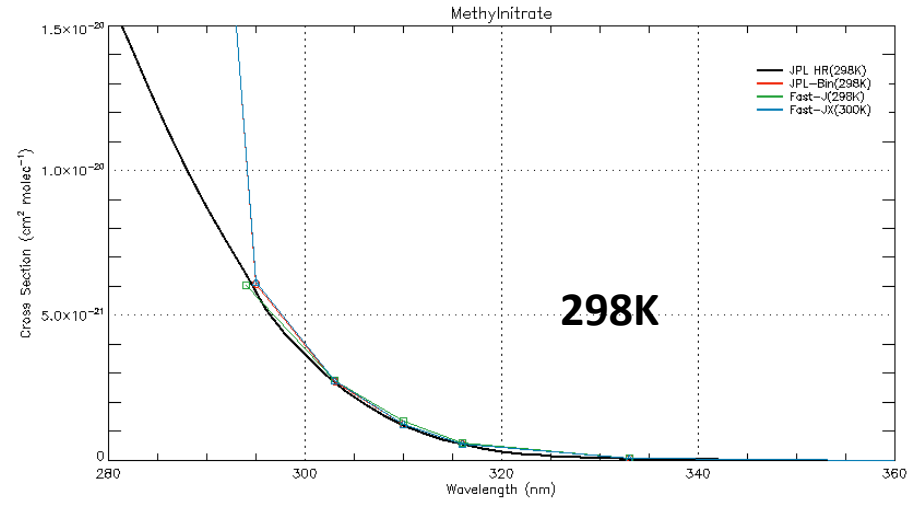
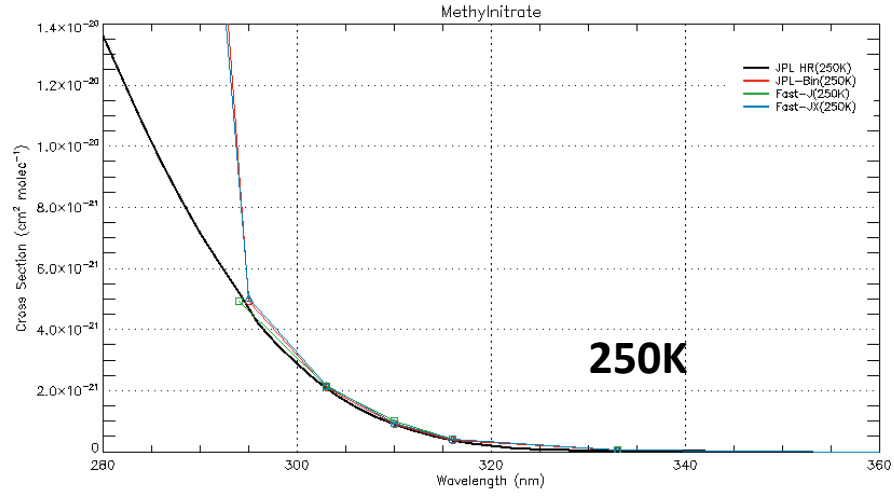
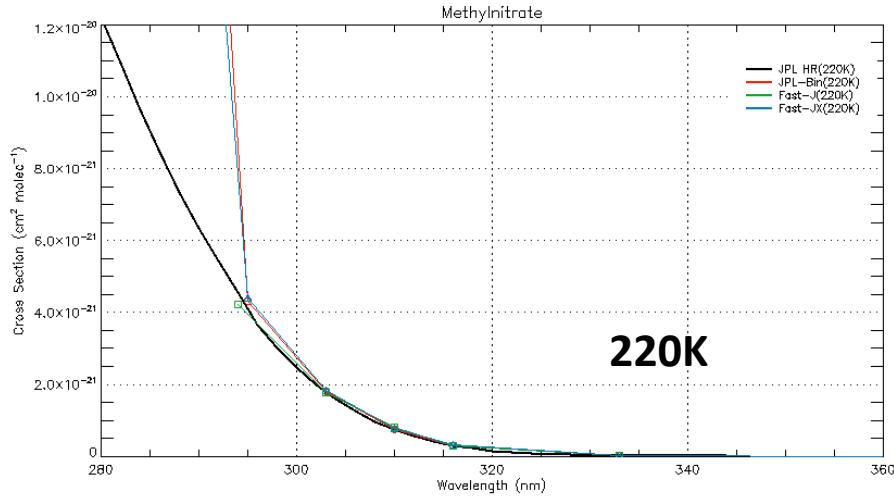
4D-18

$$\sigma(\lambda, T) = \sigma(\lambda, 298 \text{ K}) \times \exp[B(\lambda)(T - 298)]$$

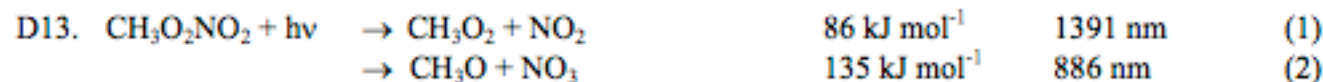
Photolysis Quantum Yields and Product Studies: The photodissociation quantum yield for CH_3ONO_2 to produce NO_2 and CH_3O was measured by Talukdar et al. [186] to be $\Phi_1 = 0.91 \pm 0.20$ at 248 nm. Upper limits for the other channels were determined experimentally to be $\Phi_2 < 0.05$, $\Phi_3 < 0.005$, $\Phi_{4+8} < 0.1$ and $\Phi_5 < 0.015 \pm 0.01$. It is expected that the quantum yield Φ_1 is unity at wavelengths >248 nm. Oxygen atoms were measured with quantum yield of 0.65 ± 0.15 at 193 nm and <0.01 at 248 and 308 nm. Yang et al. [209] studied the photodissociation of jet-cooled CH_3ONO_2 at 193 and 248 nm and found channel (1) to be the principal photolysis product channel with relative yields of 0.7 and 1 at 193 and 248 nm, respectively. They also reported an $\text{O}(^1\text{D})$ yield of 0.3 at 193 nm.

Applies to: R4N2

D12 R4N2



D13 - MPN



(Recommendation: 10-6, Note: 10-6, Evaluated: 10-6)

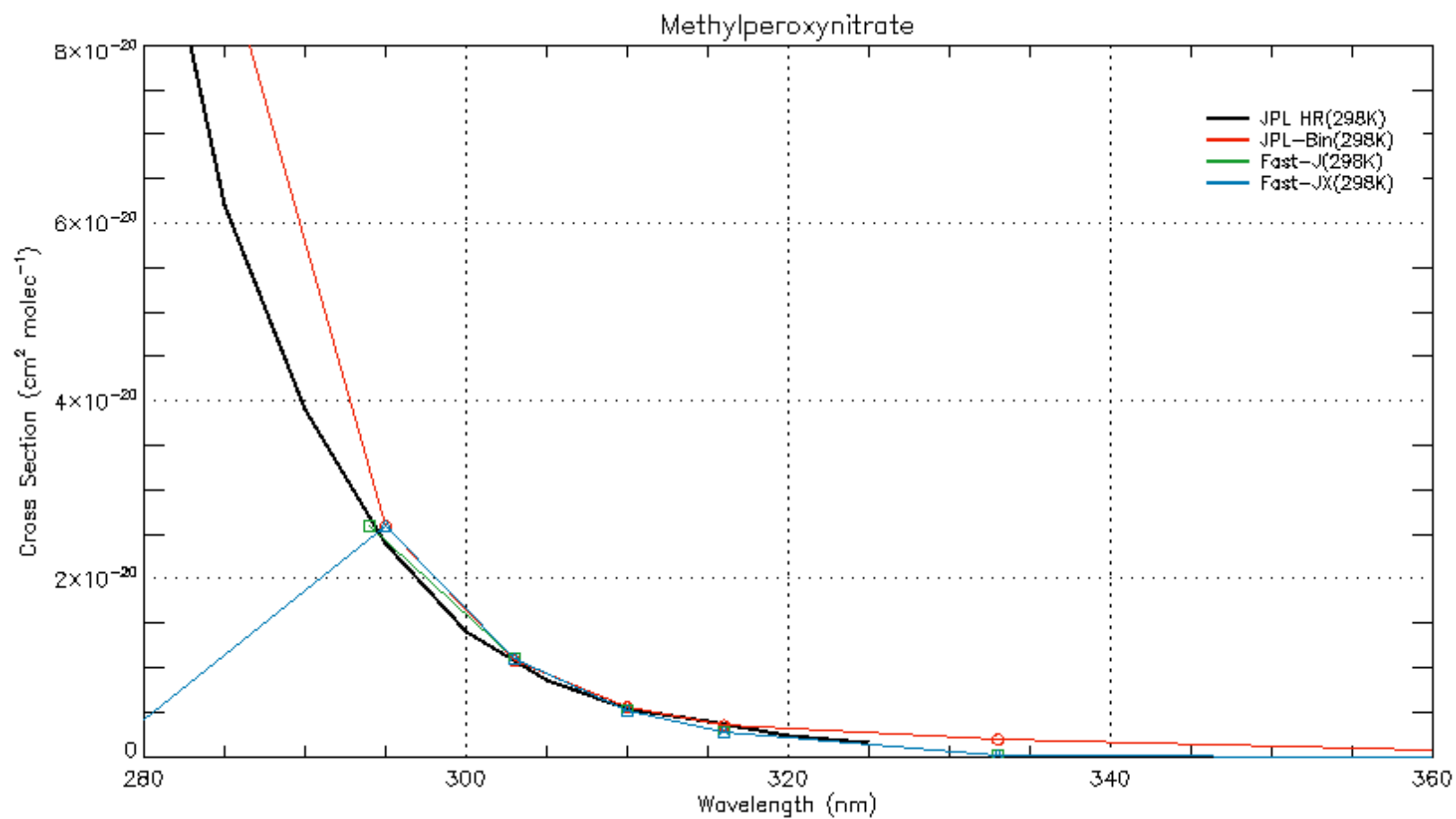
Absorption Cross Sections: The UV absorption spectrum of $\text{CH}_3\text{O}_2\text{NO}_2$ (methylperoxynitrate) has been measured by Cox and Tyndall [51] (200 – 310 nm) at 275 K, Morel et al. [143] (200 – 290 nm) at 296 K, Sander and Watson [170] (240 – 280 nm) at 298 K, and Bridier et al. [28] (200 – 280 nm) at 298 K. The spectrum has a strong absorption band below 225 nm and a moderate band at longer wavelengths. The reported cross sections are in reasonable agreement in the range 230 – 250 nm but scatter in the cross section data exists at both shorter and longer wavelengths. The recommended cross sections listed in Table 4D-16 are a smoothed average of the data from the four studies.

4D-19

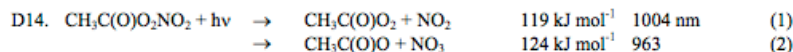
Photolysis Quantum Yields and Product Studies: No studies are available.

Applies to: MPN

D13 - MPN



D14 - PAN



(Recommendation: 06-2, Note 10-6, Evaluated 10-6)

Absorption Cross Sections. The absorption cross sections of $\text{CH}_3\text{C(O)O}_2\text{NO}_2$ (peroxyacetyl nitrate, PAN) have been measured at room temperature by Stephens [183] (220 – 450 nm), Senum et al. [173] (200 – 300 nm), Basco and Parmar [15] (210 – 250 nm), and Libuda and Zabel [106] (219 – 325 nm) and at 250, 273, and 298 K by Talukdar et al. [187] (196 – 350 nm). The studies are in reasonable agreement. The data of Talukdar et al. [187] and Libuda and Zabel [106] agree within 10% at wavelengths <300 nm. The data of Stephens [183] and Basco and Parmar [15] are greater by up to 20 and 45%, respectively. The Senum et al. [173] cross sections are systematically less than the data of Talukdar et al. [187]. Libuda and Zabel [106] carried out simultaneous UV and IR studies that showed that their measured cross sections needed to be corrected for impurities that are transparent in the UV but contribute to the sample pressure in the absorption cell. The corrections were on the order of 20%. The recommended absorption cross sections listed in Table 4D-17 are taken from Talukdar et al. [187] which are in good agreement with those of Libuda and Zabel [106] but include a wider spectral coverage and temperature range. The uncertainties in the cross sections are estimated to be of the order of a factor of 2 in the long wavelength region but smaller at shorter wavelengths, decreasing to about 10% at 220 nm.

A systematic decrease of the absorption cross sections with decreasing temperature was observed by Talukdar et al. [187]. The temperature dependence was parameterized using the expression

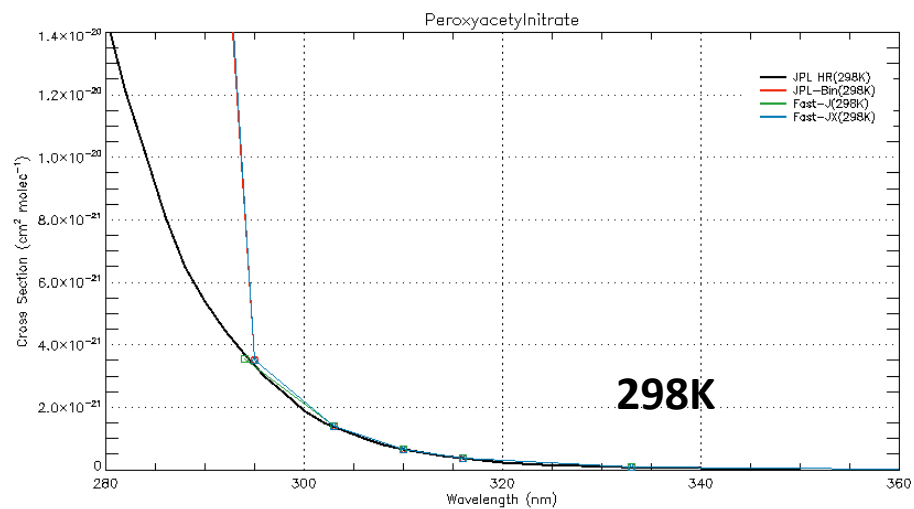
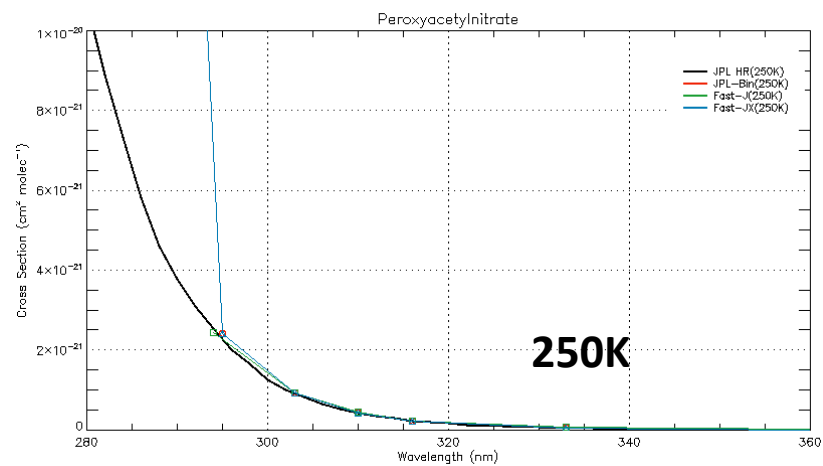
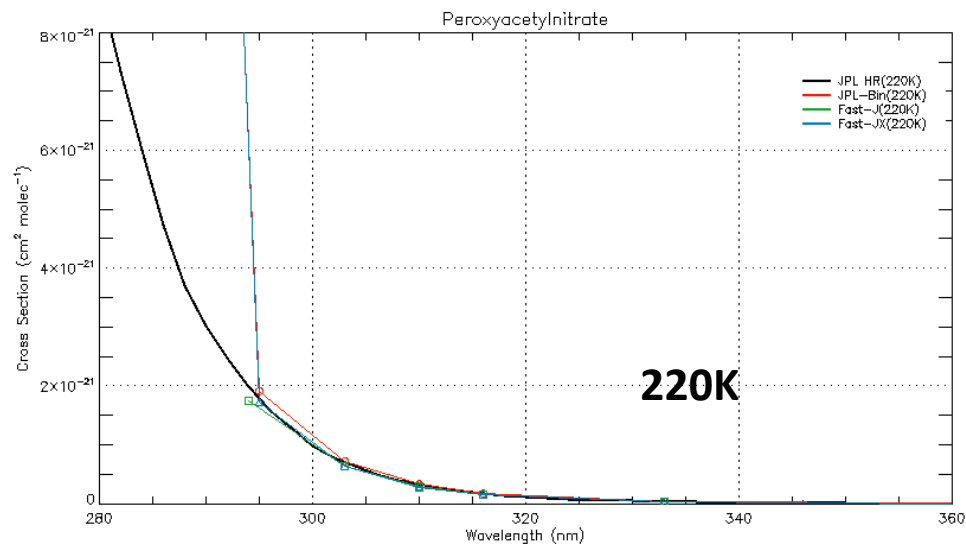
$$\ln \sigma(\lambda, T) = \ln \sigma(\lambda, 298 \text{ K}) + B(\lambda)(T - 298)$$

The temperature coefficients $B(\lambda)$ are listed in Table 4D-17.

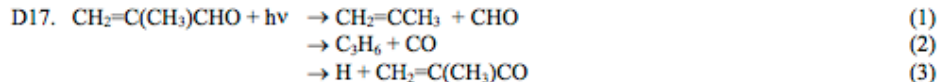
Photolysis Quantum Yields and Product Studies. Quantum yields for the production of NO_2 and NO_3 in the photolysis at 248 nm were reported by Mazely et al. [122, 123]: $\Phi(\text{NO}_2, 248 \text{ nm}) = 0.83 \pm 0.09$ and $\Phi(\text{NO}_3, 248 \text{ nm}) = 0.3 \pm 0.1$. The NO_3 quantum yield was obtained relative to the unity NO_3 quantum yield in the photolysis of N_2O_5 at 248 nm. However, this latter quantum yield was re-measured to be 0.8 ± 0.1 by Harwood et al. [77], so that the $\Phi(\text{NO}_3, 248 \text{ nm})$ should be rescaled to 0.24. Quantum yields for the production of NO_3 in the photolysis of $\text{CH}_3\text{C(O)O}_2\text{NO}_2$ at 248 and 308 nm were also measured by Harwood et al. [78]: $\Phi(\text{NO}_3, 248 \text{ nm}) = 0.19 \pm 0.04$ and $\Phi(\text{NO}_3, 308 \text{ nm}) = 0.41 \pm 0.10$. Flowers et al. [64] studied the photolysis of PAN at 289 nm and detected NO_3 using cavity ring-down spectroscopy. They obtained $\Phi(\text{NO}_3, 289 \text{ nm}) = 0.31 \pm 0.08$ relative to the unity NO_3 quantum yield in the photolysis of N_2O_5 . In a second study, Flowers et al. [65] measured the wavelength dependence of $\Phi(\text{NO}_3)$: at 294 nm (0.29 ± 0.07), 299 nm (0.28 ± 0.07), 308 nm (0.28 ± 0.05), and 312 nm (0.39 ± 0.07). These results indicate that between 289 and 308 nm the NO_3 quantum yield is nearly constant with $\Phi(\text{NO}_3) = 0.29 \pm 0.07$. An increase of $\Phi(\text{NO}_3)$ at longer wavelengths cannot be ruled out. The recommended quantum yields are $\Phi(\text{NO}_2) = 0.7$ and $\Phi(\text{NO}_3) = 0.3$ for $\lambda > 300 \text{ nm}$.

Applies to: PAN

D14 - PAN



D17 - MACR



(Recommendation: 06-2, Note: 10-6, Evaluated: 10-6)

Absorption Cross Sections: The VUV/UV absorption spectrum of methacrolein (2-methylpropenal, MACR), $\text{CH}_2=\text{C}(\text{CH}_3)\text{CHO}$, has been measured using diode array spectroscopy at room temperature by Meller (237 – 391 nm) (see Röth et al. [169]), Raber and Moortgat [161] (331 nm), Gierczak et al. [71] (214, 250 – 395 nm), and Lee et al. [103]. The spectrum exhibits a broad absorption band between 250 and 390 nm with vibrational structure above 310 nm. A detailed vibrational-electronic analysis was reported by Birge et al. [20]. The reported spectra are in very good agreement in the region 261-351 nm where the agreement is between ~1 and 10%. At shorter wavelengths, <260 nm, the differences increase to nearly 100% at 250 nm and the cross sections from Gierczak et al. [71] are consistently greater than those of Meller [169] and Raber and Moortgat [161]. The cross sections at the peaks in the structured region reported by Meller [169] and Raber and Moortgat [161] are consistently higher than those measured by Gierczak et al. [71] presumably due to the higher resolution used. At the band maximum, Raber and Moortgat [161] reported $\sigma(330.7 \text{ nm}) = 7.64 \times 10^{-20} \text{ cm}^2 \text{ molecule}^{-1}$ and Gierczak et al. [71] reported $\sigma(331 \text{ nm}) = 7.2 \times 10^{-20} \text{ cm}^2 \text{ molecule}^{-1}$. Gierczak et al. [71] also reported $\sigma(213.86 \text{ nm}) = (2.21 \pm 0.11) \times 10^{-17} \text{ cm}^2 \text{ molecule}^{-1}$ (Zn lamp source). The 1 nm averages of the results from Gierczak et al. [71] and Meller [169] are generally (with a few exceptions) within 20% of each other for wavelengths up to 376 nm. Above 380 nm, the results of Gierczak et al. [71] are larger with increasing wavelength by up to nearly 80% than the results of Meller [169]. A wavelength shift of ~1 nm toward longer wavelengths can be observed above 340 nm in the absorption spectrum of Gierczak et al. [71] when compared to the spectrum reported by Meller [169]. The recommended absorption cross sections listed in Table 4D-20 are from Gierczak et al. [71].

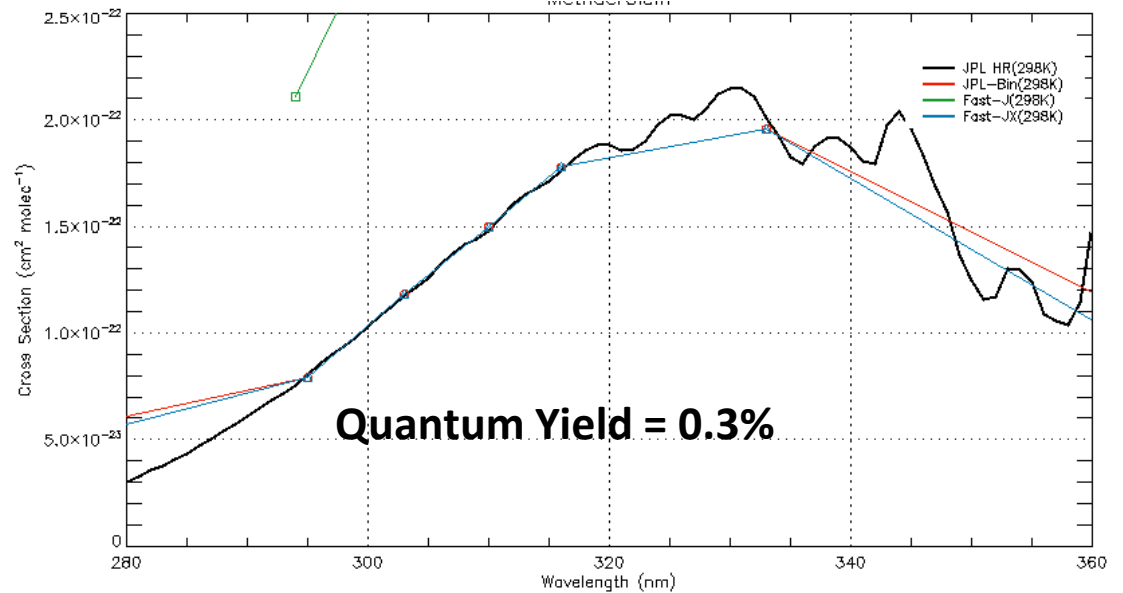
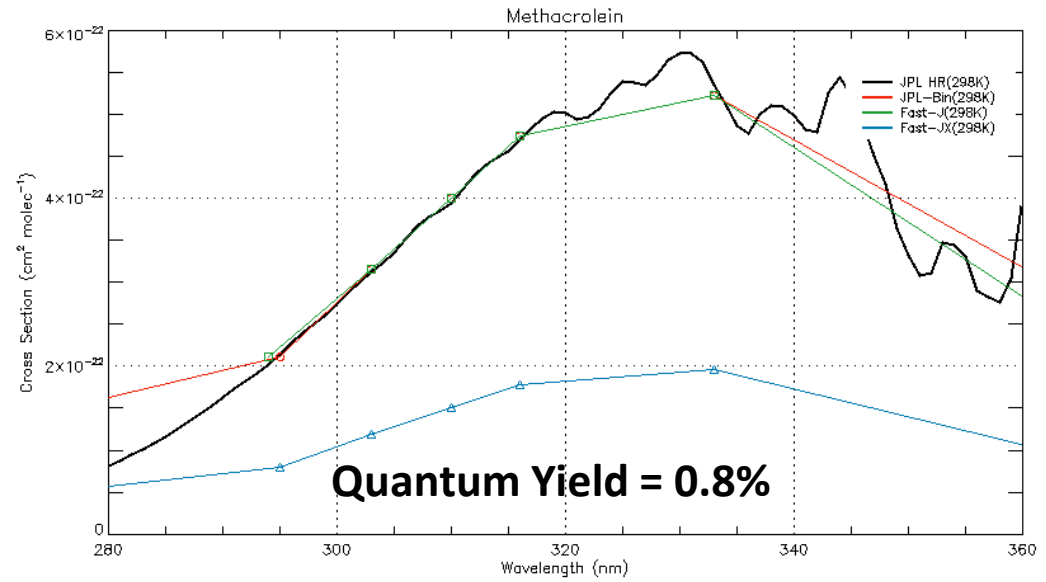
Photolysis Quantum Yield and Product Studies: The photodissociation quantum yield for $\text{CH}_2=\text{C}(\text{CH}_3)\text{CHO}$ at atmospherically relevant wavelengths is low. Quantum yields of $\text{CH}_2=\text{C}(\text{CH}_3)\text{CHO}$ were measured by Raber and Moortgat [161] using broad band photolysis in the wavelength range 275-380 nm, and determination of the stable products (CO , CO_2 , HCHO , C_2H_4 , C_3H_6 , C_2H_2) by FTIR spectroscopy. An upper limit of 0.05 was reported at 760 Torr. Gierczak et al. [71] used GC and GC-MS detection of photolysis end-

4D-23

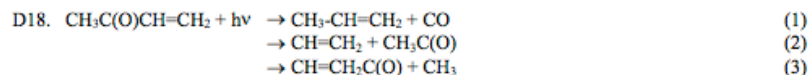
Applies to: MACR

products to determined $\text{CH}_2=\text{C}(\text{CH}_3)\text{CHO}$ quantum yields at 308 nm of 0.008 ± 0.001 and 0.005 ± 0.001 at 25 and 650 Torr total pressure, respectively. At 351 nm they reported quantum yields of 0.005 ± 0.002 and 0.003 ± 0.001 at 25 and 650 Torr, respectively. A value of $\Phi < 0.01$ is recommended for wavelengths >308 nm.

D17 - MACR



D18 - MVK



(Recommendation: 06-2, Note: 10-6, Evaluated: 10-6)

Absorption Cross Sections: The UV absorption spectrum of methyl vinyl ketone (MVK), $\text{CH}_3\text{C(O)CH=CH}_2$, has been measured at room temperature by Schneider and Moortgat (240 – 398 nm) (see Röth et al. [169]), Raber and Moortgat [161] (235 – 400 nm), Fahr et al. [59] (160 – 260 nm), and Gierczak et al. [71] (216.86 nm and 250 – 395 nm). The absorption band peaking at ~330 nm displays some weak vibrational band structure, which is superimposed on a continuum envelope. A detailed vibrational-electronic analysis was reported by Birge et al. [20]. The cross sections from Schneider and Moortgat are somewhat smaller around

4D-25

the band maximum at 334 nm (agreement within ~10% between 290 and 365 nm), and larger by up to 50% and smaller by up to ~60% in the short- and long-wavelength tails, respectively, than the results of Gierczak et al. [71]. Gierczak et al. [71] reported $\sigma(213.86 \text{ nm}) = (6.6 \pm 0.04) \times 10^{-17} \text{ cm}^2 \text{ molecule}^{-1}$ (Zn lamp source). They also measured the spectrum at reduced temperatures (range 250 – 298 K), and observed a small increase in the peak cross section of <2% at 250 K. Fahr et al. [59] reported $\sigma(193 \text{ nm}) = (3.2 \pm 0.2) \times 10^{-17} \text{ cm}^2 \text{ molecule}^{-1}$. The recommended absorption cross sections in Table 4D-21 are taken from Gierczak et al. [71].

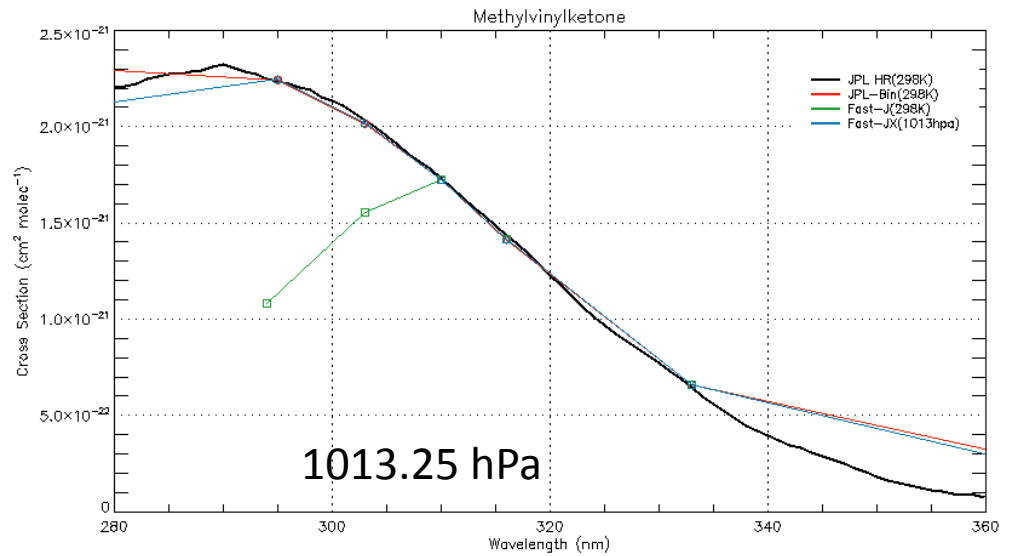
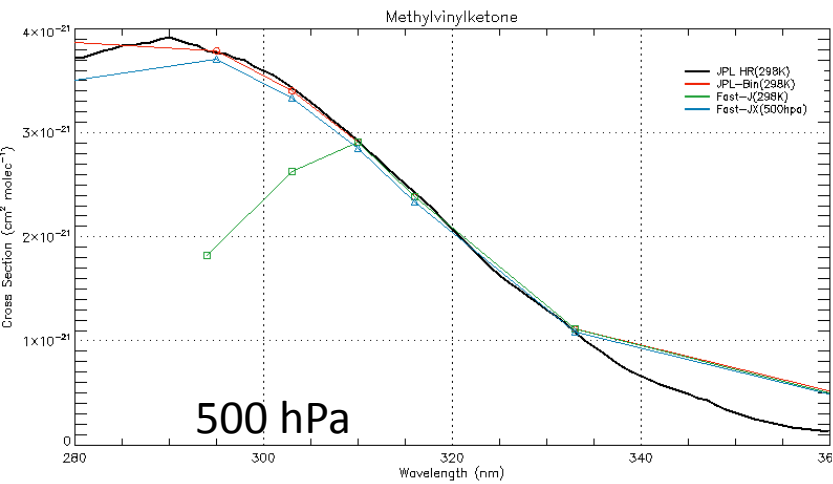
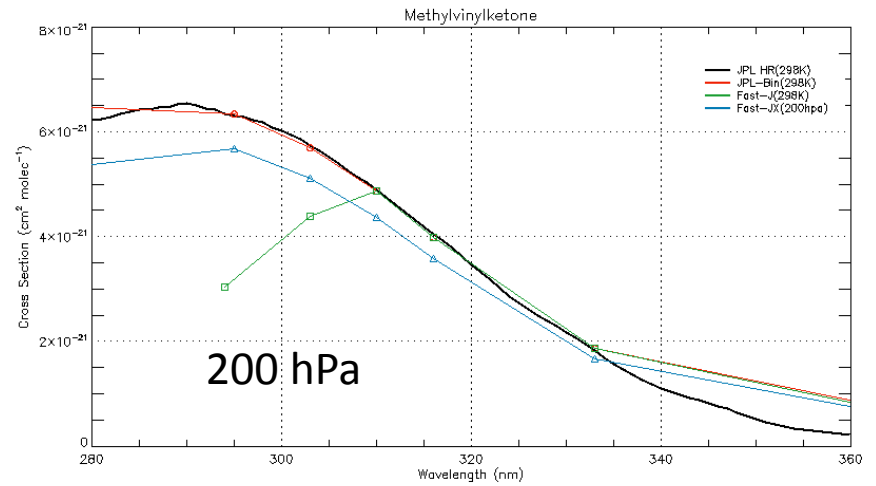
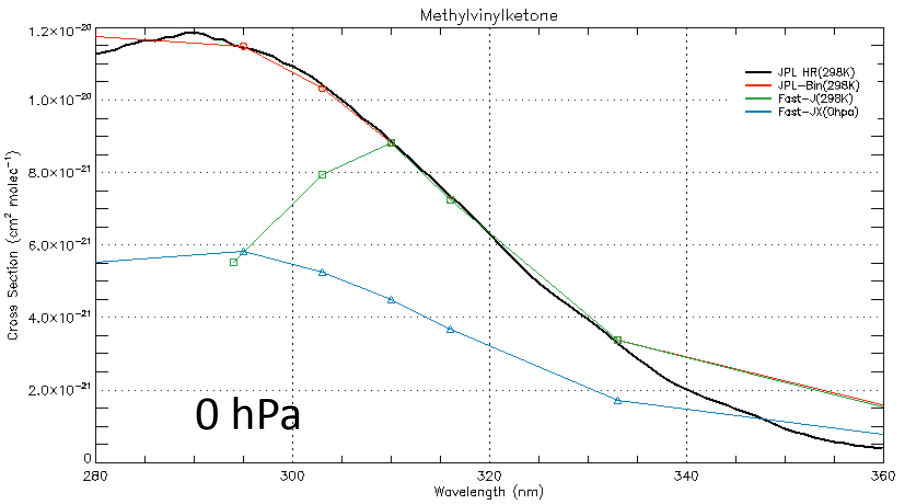
Photolysis Quantum Yield and Product Studies: Product quantum yields were measured by Raber and Moortgat [161] using broadband photolysis in the range 275 – 380 nm combined with FTIR monitoring of the stable photolysis products (major CO, C_3H_6 and HCHO; minor CO_2 , HCOOH, CH_2OH , CH_3COOH). They report a pressure dependent quantum yield with $\Phi = 0.05$ at 760 Torr and $\Phi = 0.12$ at 54 Torr. Fahr et al. [59] used laser photolysis at 193.3 nm and measured the direct formation of CH_3 radicals at 216.4 nm and final products. They report a quantum yield close to unity for the formation of CH_3 and CH=CH_2 radicals. Gierczak et al. [71] measured quantum yields for photolysis at 308, 337 and 351 nm by monitoring the disappearance of MVK. They reported $\Phi = 0.16$ at 25 Torr and $\Phi = 0.04$ at 760 Torr at 308 nm, $\Phi = 0.04$ at 25 Torr and $\Phi = 0.01$ at 760 Torr at 337 nm; and $\Phi = 0.01$ independent of pressure at 351 nm. The quantum yield data were fit to the empirical Stern-Volmer type expression

$$\Phi(\lambda, P) = \exp[-0.055(\lambda - 308)] / (5.5 + 9.2 \times 10^{-19} [M])$$

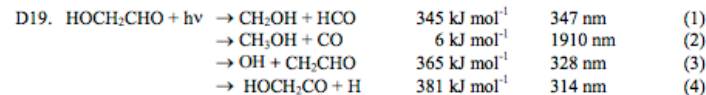
where λ is in nm and $[M]$ in molecule cm^{-3} . This parameterization is recommended.

Applies to: MVK

D18 - MVK



D19 - GLYC



(Recommendation: 10-6, Note: 10-6, Evaluated: 10-6)

Absorption Cross Sections: The absorption cross sections of HOCH₂CHO (glycolaldehyde, hydroxyacetaldehyde) have been measured at room temperature by Bacher et al. [13] (205 – 335 nm), Magneron et al. [112] (210 – 330 nm), and Karunanandan et al. [94] (210 – 335 nm). The spectrum consists of a strong absorption below 220 nm and a weaker absorption band centered near 280 nm with evidence of

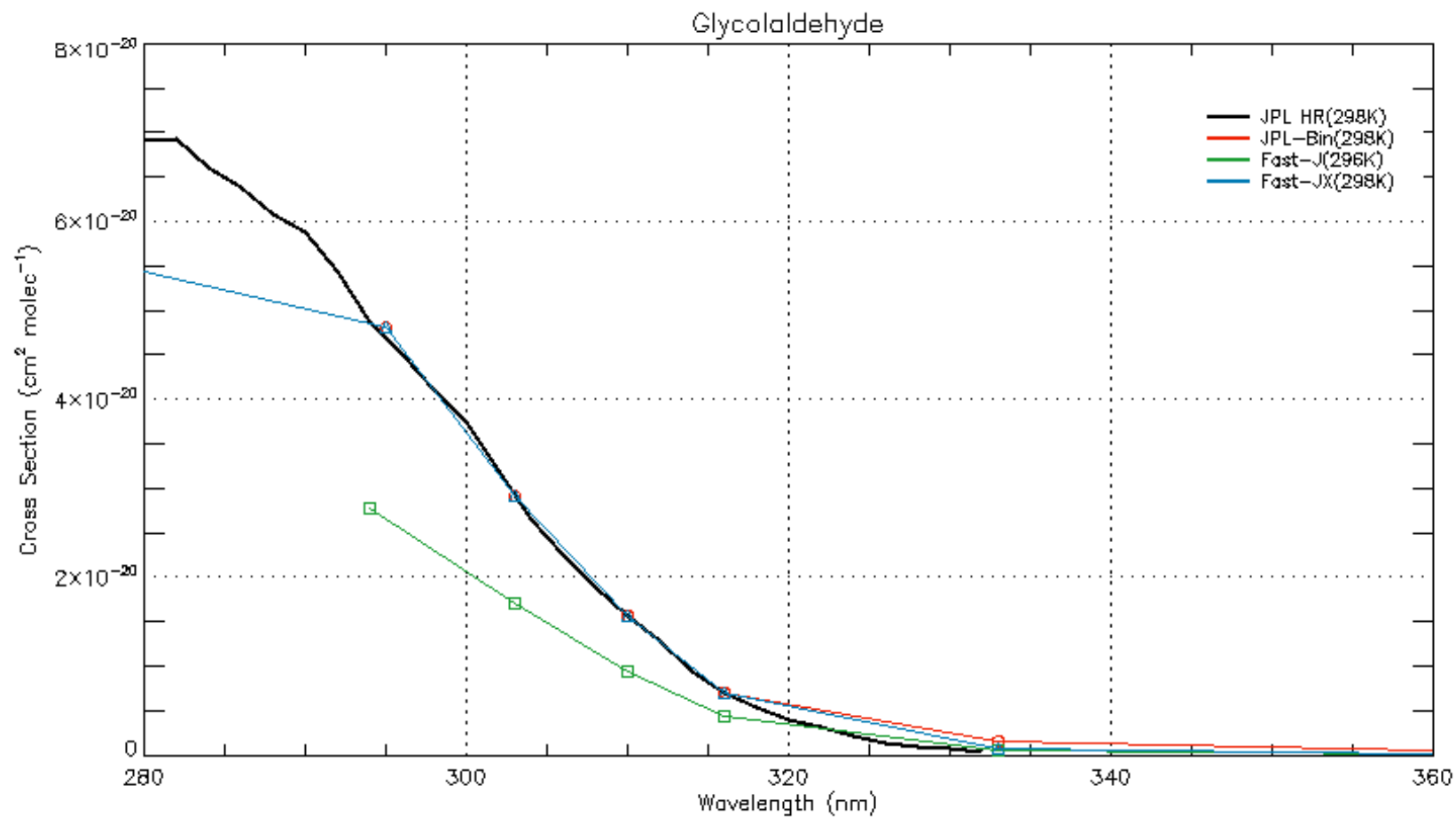
4D-27

vibrational progressions. The measurements performed by Magneron et al. [112] were done at two different laboratories and are nearly identical but reveal significant differences compared to the spectrum measured by Bacher et al. [13], being about 20% at the maximum. The spectrum measured by Karunanandan et al. [94] is in excellent agreement with Magneron et al. [112] at the maximum near 282 nm and at longer wavelengths. At shorter wavelengths the cross sections are consistently larger than those measured by Magneron et al. [112]: 15% at 250 nm, 40% at 230 nm and 85% at the minimum near 226 nm. At 184.9 nm the cross section was measured as $(3.85 \pm 0.2) \times 10^{-18} \text{ cm}^2 \text{ molecule}^{-1}$. The average of the cross sections of Magneron et al. [112] and Karunanandan et al. [94] are recommended and listed in Table 4D-22.

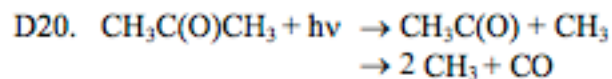
Photolysis Quantum Yields and Product Studies: The broad band photolysis ($285 \pm 25 \text{ nm}$) of glycolaldehyde in air performed by Bacher et al. [13] revealed an overall quantum yield $\Phi > 0.5$, relative to the quantum yield ($\Phi = 0.3$) of removal of acetone. Product studies by FTIR suggests that channel (1) is the major photolysis channel (65-80%), while channel (2) accounts to 15-20%, and channel (3) contributes up to 15%. The formation of channel (4) was suggested to produce HOCH₂CO as a source for OH radicals, whose presence was indirectly invoked due the formation of glyoxal. Magneron et al. [112] also photolysed glycolaldehyde (broadband lamps 275 – 380 nm) and measured products by FTIR (CO, CO₂, HCHO and CH₃OH). They observed direct evidence for OH production via channel (3) using OH scavenger and OH tracer species and performed additional photolysis experiments where glycolaldehyde was used an OH source to measure rate constants for OH with a series of dienes. The contribution of channel (2) was estimated to be 10% and that of channels (1) + (2) to be 90%. No evidence was found for channel (4). Karunanandan et al. [94] measured a quantum yield of OH formation at 248 nm of $\Phi_3 = (7.0 \pm 1.5) \times 10^{-2}$. On the basis of the combined product studies the following quantum yields are recommended: $\Phi_1 = 0.83$, $\Phi_2 = 0.10$ and $\Phi_3 = 0.07$ in the range 248 – 328 nm.

Applies to: GLYC

D19 - GLYC



D20 - ACET



$$354 \text{ kJ mol}^{-1} \quad 338 \text{ nm} \quad (1)$$

$$400 \text{ kJ mol}^{-1} \quad 299 \text{ nm} \quad (2)$$

Cross Section (2nd eqn)

$$\sigma(\lambda, T) = \sigma(\lambda, 298 \text{ K})[1 + c_1(\lambda)T + c_2(\lambda)T^2]$$

that was later superseded by Burkholder [31] using the expression

$$\sigma(\lambda, T) = \sigma(\lambda, 298 \text{ K})[1 + A(\lambda)T + B_2(\lambda)T^2 + C(\lambda)T^3]$$

The recommended absorption cross sections at 298 K in Table 4D-23 are taken from Gierczak et al. [70] and the temperature coefficients A, B, and C derived by Burkholder [31].

The quantum yield data of Blitz et al. [24, 25] are recommended. The optimized parameterization of the quantum yields for the wavelength range 279 – 327.5 nm, temperature range 218 – 295 K and pressure range 0 – 1000 mbar is as follows:

$$\Phi_{\text{TOTAL}}(\lambda, [M], T) = \Phi_{\text{CH}_3\text{CO}}(\lambda, [M], T) + \Phi_{\text{CO}}(\lambda, T); \quad \text{all } \lambda$$

For $\lambda = 279\text{-}327.5 \text{ nm}$

$$\Phi_{\text{CO}}(\lambda, T) = 1 / (1 + A_0)$$

$$\text{where } A_0 = [a_0 / (1 - a_0)] \exp[b_0 \{\lambda - 248\}]$$

$$a_0 = (0.350 \pm 0.003) (T/295)^{(-1.28 \pm 0.03)}$$

$$b_0 = (0.068 \pm 0.002) (T/295)^{(-2.65 \pm 0.20)}$$

For $\lambda = 279\text{-}302 \text{ nm}$

$$\Phi_{\text{CH}_3\text{CO}}(\lambda, [M], T) = \{1 - \Phi_{\text{CO}}(\lambda, T)\} / \{1 + A_1[M]\}$$

$$\text{where } A_1 = a_1 \exp[-b_1 \{(10^7/\lambda) - 33113\}]$$

$$a_1 = (1.600 \pm 0.032) \times 10^{-19} (T/295)^{(-2.38 \pm 0.08)}$$

$$b_1 = (0.55 \pm 0.02) \times 10^{-3} (T/295)^{(-3.19 \pm 0.13)}$$

For $\lambda = 302\text{-}327.5 \text{ nm}$,

$$\Phi_{\text{CH}_3\text{CO}}(\lambda, [M], T) = \{(1 + A_4[M] + A_3) / [(1 + A_2[M] + A_3)(1 + A_4[M])]\} \{1 - \Phi_{\text{CO}}(\lambda, T)\}$$

$$\text{where } A_2 = a_2 \exp[-b_2 \{(10^7/\lambda) - 30488\}]$$

$$a_2 = (1.62 \pm 0.06) \times 10^{-17} (T/295)^{(-10.03 \pm 0.20)}$$

$$b_2 = (1.79 \pm 0.02) \times 10^{-3} (T/295)^{(-1.364 \pm 0.036)}$$

$$A_3 = a_3 \exp[-b_3 \{(10^7/\lambda) - c_3\}^2]$$

$$a_3 = (26.29 \pm 0.88) (T/295)^{(-6.59 \pm 0.23)}$$

$$b_3 = (5.72 \pm 0.20) \times 10^{-7} (T/295)^{(-2.93 \pm 0.09)}$$

$$c_3 = (30006 \pm 41) (T/295)^{(-0.064 \pm 0.004)}$$

$$A_4 = a_4 \exp[-b_4 \{(10^7/\lambda) - 30488\}]$$

$$a_4 = (1.67 \pm 0.14) \times 10^{-15} (T/295)^{(-7.25 \pm 0.54)}$$

$$b_4 = (2.08 \pm 0.02) \times 10^{-3} (T/295)^{(-1.16 \pm 0.15)}$$

Applies to: ACET

where [M] is in molecule cm^{-3} , λ in nm and T in K. The equations given above have been used to calculate the quantum yields given in Table 4D-24.

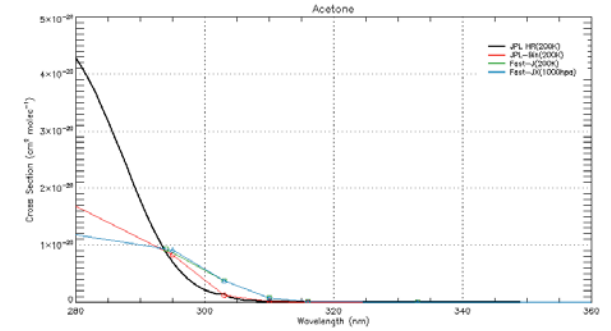
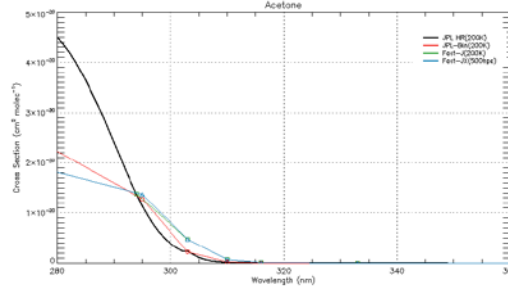
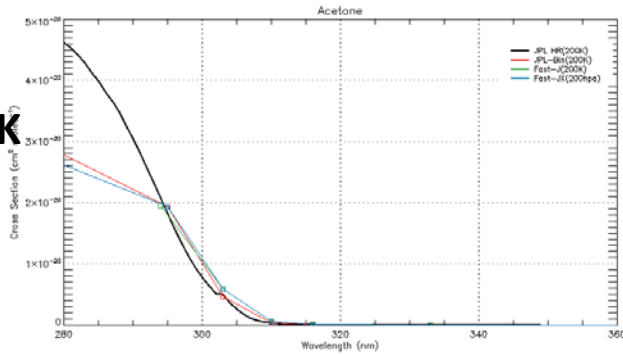
D2O - ACET

200 hpa

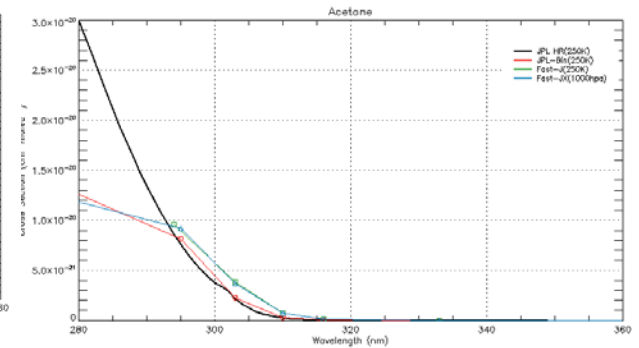
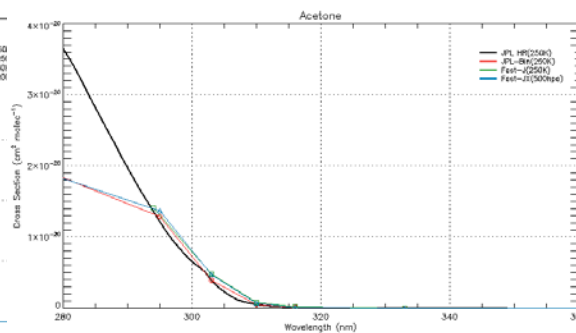
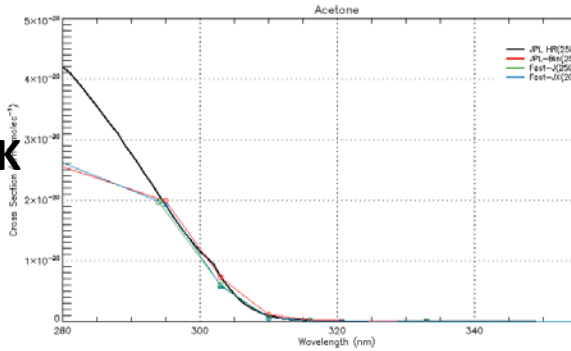
500 hpa

1000 hpa

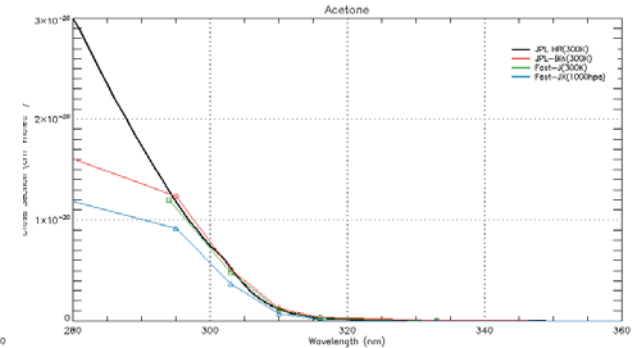
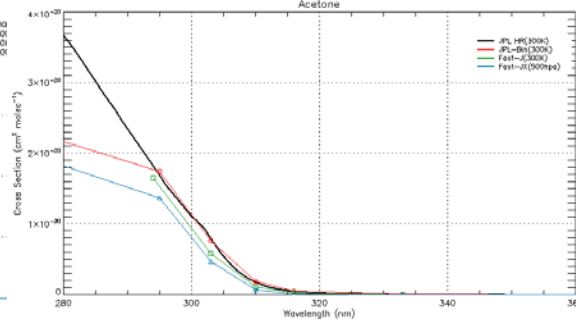
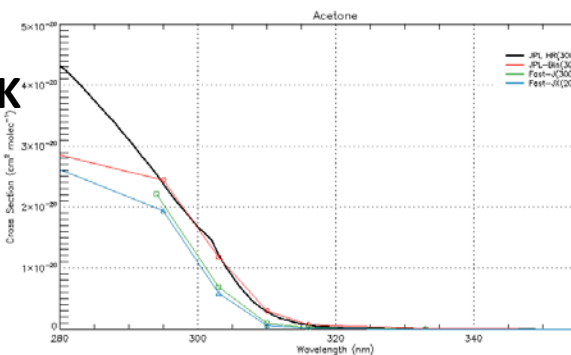
200K



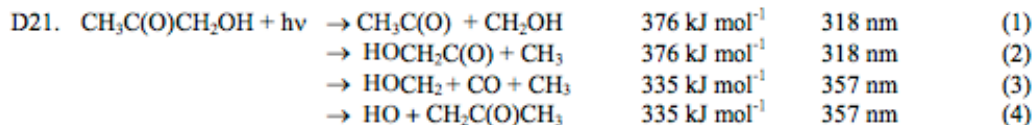
250K



300K



D21 - HAC



(Recommendation: 10-6, Note: 10-6, Evaluated: 10-6)

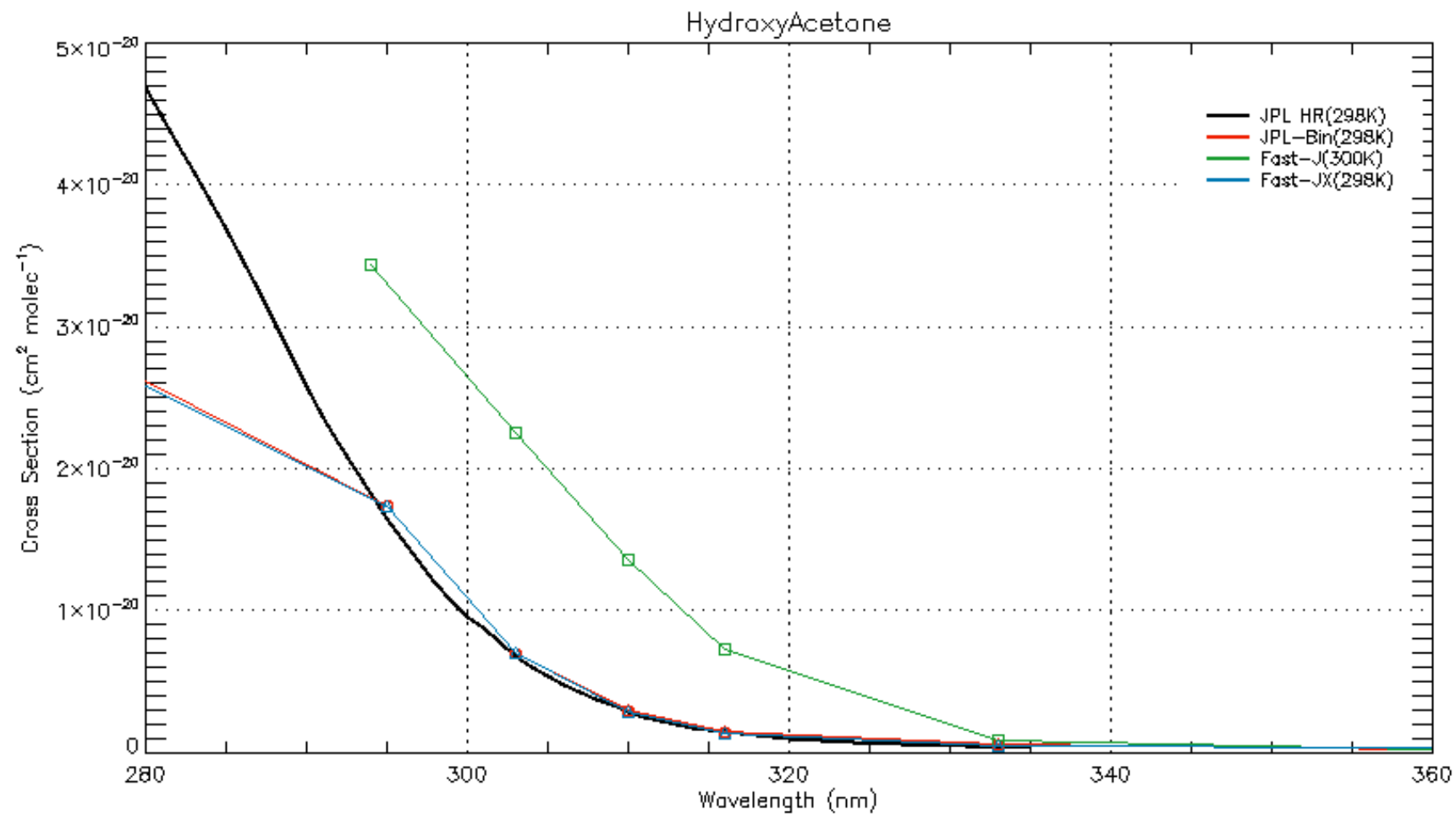
Absorption Cross Sections: The absorption cross sections of $\text{CH}_3\text{C}(\text{O})\text{CH}_2\text{OH}$ (hydroxyacetone, acetol) have been measured by Meller and Crowley [127] at 296 K in the range 207 – 333 nm; by Orlando et al. [152] at 298 K over the range 235 – 340 nm; and by Butkovskaya et al. [32] at 294 K over the range 240 – 350 nm using a static method, and at 328 K over the range 250 – 350 nm using a dynamic method. Dillon et al. [55] measured the cross section at 184.9 nm and 358 K to be $(5.4 \pm 0.1) \times 10^{-18} \text{ cm}^2 \text{ molecule}^{-1}$ whereas Baasandorj et al. [12] reported a value of $(5.43 \pm 0.08) \times 10^{-18} \text{ cm}^2 \text{ molecule}^{-1}$ at 298 K. The spectrum shows an absorption band with the maximum near 266 nm. The shape of the measured spectra are in excellent agreement except for the spectrum obtained by Butkovskaya et al. [32] using the dynamic method. The maxima cross sections reported by Butkovskaya et al. [32] are 15% and 24% lower for the static and dynamic methods, respectively, than the values obtained by Orlando et al. [152]; the maximum reported by Meller and Crowley [127] is 11% lower than that of Orlando et al. [152]. Large discrepancies between the measured spectra exist at $\lambda > 310 \text{ nm}$.

In Table 4D-25 are listed the averages over 1 nm intervals of the cross sections of Orlando et al. [152] and Butkovskaya et al. [32] (static) in the wavelength range 240 – 310 nm; at 311 – 336 nm, only those of Orlando et al. [152].

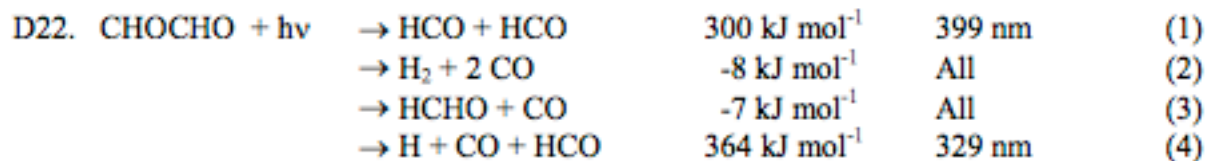
Photolysis Quantum Yield and Product Studies: Quantum yields for removal of hydroxyacetone were estimated by Orlando et al. [152] to be 0.65 ± 0.25 for the photolysis in the 240 – 420 nm band. They also suggested that $0.3 \pm 0.2 < \Phi_1 + \Phi_2 < 0.6$ for wavelengths larger than 290 nm. Products detected were CO , CO_2 , CH_2O , CH_3COOH , $\text{CH}_3\text{COO}_2\text{H}$, HCOOH and CH_3OH . These authors concluded that at most 50% of the photolysis occurred via channel (1). Direct observation of OH radicals, presumably arising from channel (4), was made by Chowdhury et al. [46] at 148 nm. Photolysis of hydroxyacetone at 193 nm was performed by Chowdhury et al. [46] and appears to occur by process (2) with the initial formation of HOCH_2CO yielding OH and ketene.

Applies to: HAC

D21 - HAC



D22 - GLYX



Photolysis Quantum Yield and Product Studies: The photodissociation of CHOCHO as well as the photolysis product channel yields are wavelength and pressure dependent. Calvert and Pitts [37] have summarized the CHOCHO quantum yield data prior to 1966. On the basis of the work by Calvert and Layne [35] and Parmenter [156] it was established that the HCHO + CO photolysis channel (3) was the dominant photolysis channel with yields between 0.84 and 0.6 over the wavelength range 254 to 435 nm. There was little experimental evidence for the HCO + HCO radical channel (1) occurring and it was incorrectly concluded to be negligible. Plum et al. [158] has since reported the effective quantum yield for CHOCHO photolysis at wavelengths >290 nm to be 0.029, based on measured photolysis rates in an environmental chamber relative to NO₂ where J_{CHOCHO}/J_{NO₂} was found to be 0.008 ± 0.005. An effective atmospheric photolysis rate was measured using solar radiation in the EUPHORE outdoor chamber to be J_{obs} = 1.04 ± 0.10 × 10⁻⁴ s⁻¹, corresponding to an effective quantum yield for glyoxal loss of 0.035 ± 0.007 [136, 137] in reasonable agreement with the value reported by Plum et al. [158].

Langford and Moore [102] measured HCO produced in the photolysis of glyoxal in 1000 Torr N₂ at 305 nm by direct HCO resonance absorption and deduced a total HCO yield of 0.8 ± 0.4 at 305 nm. Using cavity ring-down spectroscopy, Zhu et al. [213] reported HCO quantum yields of 1.5 (Φ₁ ≈ 0.75) for photolysis at 351 nm, 0.69 at 308 nm, 0.52 at 248 nm and 0.42 at 193 nm. In a later study Chen and Zhu [44] reported zero pressure HCO yields, Φ₀(λ), at 10 nm intervals, to increase from 0.50 ± 0.01 at 290 nm to a maximum of 2.01 ± 0.08 at 390 nm and to decrease to 0.74 ± 0.08 at 400 nm, 0.56 ± 0.04 at 410 nm, and 0.48 ± 0.03 at 420 nm. HCO quantum yields were found to be independent of the N₂ buffer gas pressure (10-400 Torr) for photolysis in the 290-370 nm region. In the wavelength region 380-420 nm the HCO quantum yield decreased with increasing pressure. They reported HCO quantum yields at 760 Torr N₂ to be 0.49 at 380 nm, 0.54 nm at 390 nm, 0.32 at 400 nm, 0.22 at 410 nm and 0.14 at 420 nm. Feierabend et al. [62] measured quantum yields for the production of HCO at 85 discrete wavelengths in the wavelength range 290-420 nm at pressures between 50 and 550 Torr (N₂) at 298 K using pulsed laser photolysis combined with cavity ring-down spectroscopy detection of HCO. Φ₀(λ) varied smoothly with wavelength with a maximum value of ~1.8 in the range 300 – 385 nm with values decreasing to near 0 at 420 nm and 0.4 at 290 nm. The high precision of the measurements enabled the pressure dependence of the HCO quantum yield to be determined at each wavelength using the Stern-Volmer relationship

$$\frac{1}{\Phi(\lambda, P)} = \frac{1}{\Phi_0(\lambda)} + \frac{k_q}{k_d}(\lambda) [N_2]$$

where k_q is the collisional quenching rate coefficient and k_d is the rate coefficient for the dissociation of glyoxal. The wavelength dependence of the rate coefficient ratio was fit to the expression

$$k_q/k_d(\lambda) = 2.3 \times 10^{-20} + 1.5 \times 10^{-19} \exp(-0.4 \Delta E) \quad (\text{cm}^3 \text{ molecule}^{-1})$$

where ΔE = ((28571/λ) – 72.5) (kcal mol⁻¹), λ is the photolysis wavelength (nm), and 72.5 kcal mol⁻¹ is the threshold for glyoxal photodissociation (there is a small barrier to dissociation on the triplet surface). The Φ₀(λ) values from the Feierabend et al. [62] work are in good agreement with the values reported by Chen and Zhu [44].

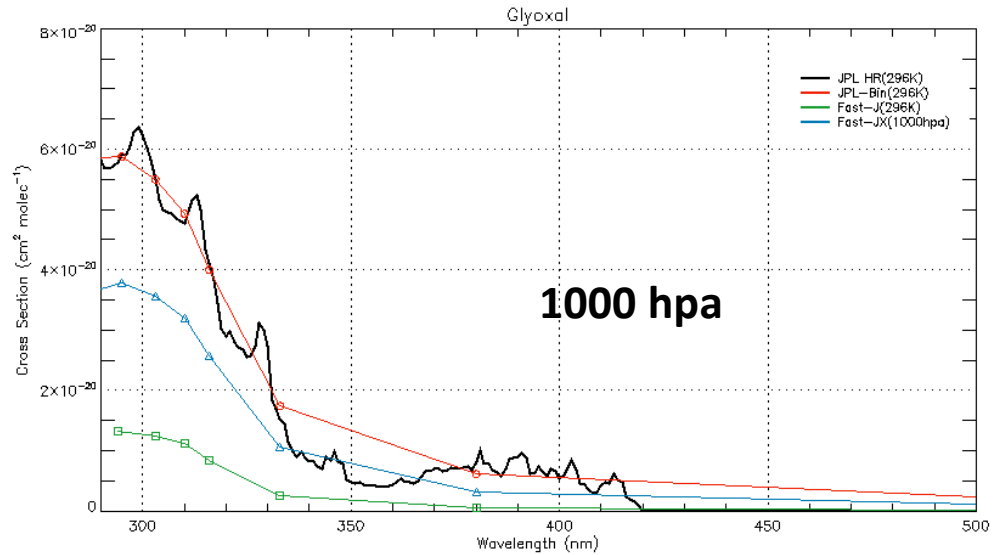
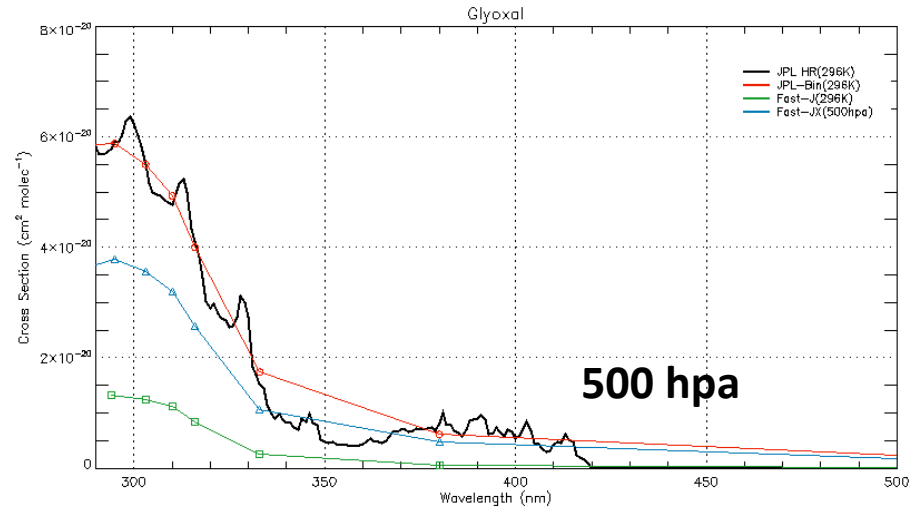
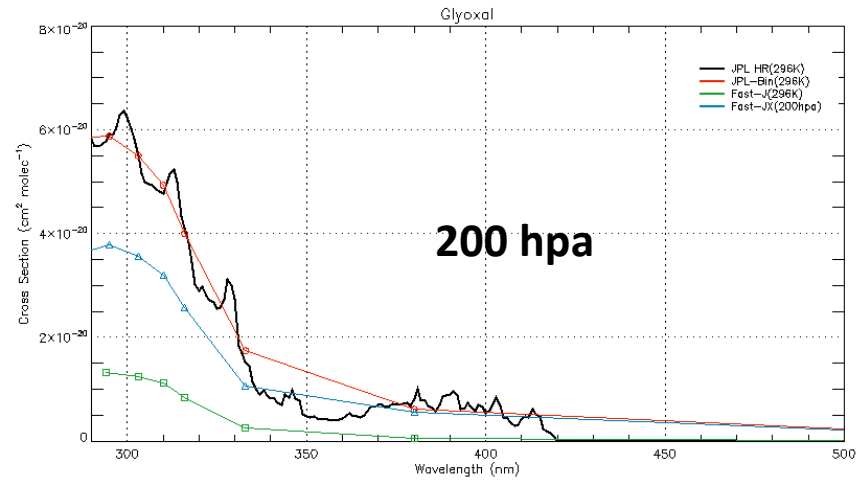
Tadić et al. [185] photolysed glyoxal with broadband fluorescent lamps, which selectively overlapped with the two absorption bands, and measured the CO, HCHO and HCOOH end products. Using 275-380 nm irradiation, the quantum yield for glyoxal loss was found to be Φ₁ = 0.97 ± 0.05 and independent of pressure. The absolute quantum yields obtained for 390 – 470 nm radiation, covering the visible absorption band, were found to be pressure dependent with values ranging from Φ_T = 0.12 at 100 Torr to Φ_T = 0.04 at 700 Torr and was described by the Stern-Volmer expression

$$\frac{1}{\Phi_T} = 6.80 + [251.8 \times 10^{-4} P(\text{Torr})]$$

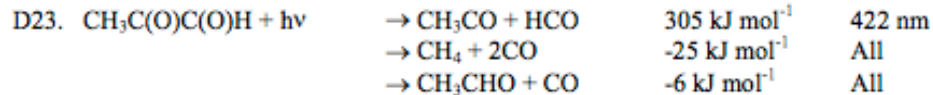
The direct HCO quantum yield measurements of Feierabend et al. [62] and Chen and Zhu [44] combined with the end product yield results of Tadić et al. [185] indicate that dissociation into 2 HCO radicals is the most important pathway under atmospheric conditions. On the basis of their HCO quantum yield data, Feierabend et al. reported a set of revised wavelength dependent quantum yields for channels (1), (2) and (3) from those of Tadić et al. [185], which were recommended in JPL 06-2. The revised quantum yields are recommended and given in Table 4D-27. Although glyoxal has a very low effective quantum yield, photolysis remains an important removal path in the atmosphere.

Applies to: GLYX

D22 - GLYX



D23 - MGLY



(1) The temperature dependence of the absorption spectrum is relatively weak with changes on the order of 10% observed in the spectrum measured by Staffelbach et al. [182] between 298 and 248 K. The largest changes occur in the structured region between 410 and 450 nm where the fine structure becomes more pronounced at lower temperatures.

(2) *Photolysis Quantum Yield and Product Studies:* Quantum yields have been measured in several studies. Kyle and Orchard [100] reported products formed in the photolysis of methylglyoxal at 387 K and 436 nm. Staffelbach et al. [182] reported a determination of products after photolysis of dilute mixtures of methylglyoxal in air using a Xe arc equipped with different band pass filters to isolate several regions of the spectrum. The observed products (CO , CO_2 , HCHO , CH_3COOH , CH_3COOOH , CH_3OH and HCOOH) led to the conclusion that only channel (1) is important in the photolysis range 240 – 480 nm. Quantum yields were derived by modeling the products formed using a number of secondary radical reactions. At 760 Torr, the Φ_1 yields were: 0.005 for the wavelength region 410 – 418 nm, 0.055 for 355 – 480 nm, 0.07 for 280-240 nm and 0.14 for 240 – 420 nm. Raber and Moortgat [161] irradiated methylglyoxal in air at different total pressures using two types of broadband lamps and determined the products (CO , CO_2 , HCHO , CH_3OOH , CH_3OH , HCOOH , CH_3CHO , CH_3COOH , CH_3COOOH and CH_3COCOOH). The quantum yield derived by modeling the products of the photolysis in the 275-380 nm region varied from 0.94 ± 0.04 at 54 Torr to 0.64 ± 0.03 at 760 Torr, and in the 390 – 470 nm region from 0.41 ± 0.04 to 0.23 ± 0.02 .

Koch and Moortgat [97] determined the quantum yields of CO , HCHO and CH_3CHO formation at 298 K as a function of wavelength (260 – 440 nm) and pressure of synthetic air (30 – 900 Torr) using “broad” monochromatic light, with an optical resolution of 8.5 nm. For photolysis in the 260 – 320 nm band, the overall quantum yield was found to be unity, independent of wavelength and pressure. The analysis of the data gave evidence that channel (1) is the predominant photolysis path. In the 380 – 440 nm band the quantum yield of CO showed a Stern-Volmer pressure dependence and the quantum yield of H_2CO increased with increasing methylglyoxal pressure, which was attributed to the reaction of excited methylglyoxal with ground state methylglyoxal.

The quantum yield of channel (1) over the wavelength range 250-500 nm was expressed as

$$1/\Phi_1(\lambda) = 1/\Phi_0(\lambda) + P(\text{Torr}) / k(\lambda)$$

where $\Phi_0(\lambda) = 1$ for $\lambda < 380$ nm
 $\Phi_0(\lambda) = (8.15 \pm 0.7) 10^{-9} [\exp(7131 \pm 267) / \lambda]$ for $\lambda > 380$ nm
 $k(\lambda) = (7.34 \pm 0.1) 10^{-9} [\exp(8793 \pm 300) / \lambda]$

Chen et al. [42] used a tunable dye laser to photolysed methylglyoxal at 10 nm intervals over the range 290 – 440 nm combined with detection of the primary HCO radical photolysis product using cavity ring-down spectroscopy. The HCO quantum yield was calibrated against HCO produced in the photolysis of HCHO or Cl_2/HCHO mixtures. They report the HCO quantum yield to be unity in the wavelength range 320-360 nm, 0.82 ± 0.06 at 290 nm, and to decrease at wavelengths > 370 nm to a value of 0.17 ± 0.02 at 440 nm. The HCO quantum yields were reported to be independent of pressure between 290 and 370 nm for the pressure range 10-400 Torr N_2 but to have a Stern-Volmer pressure dependence at wavelengths ≥ 380 nm given by

$$1/\Phi_0(\lambda) = 1/\Phi_0(\lambda) + k_0(\lambda) P(\text{Torr})$$

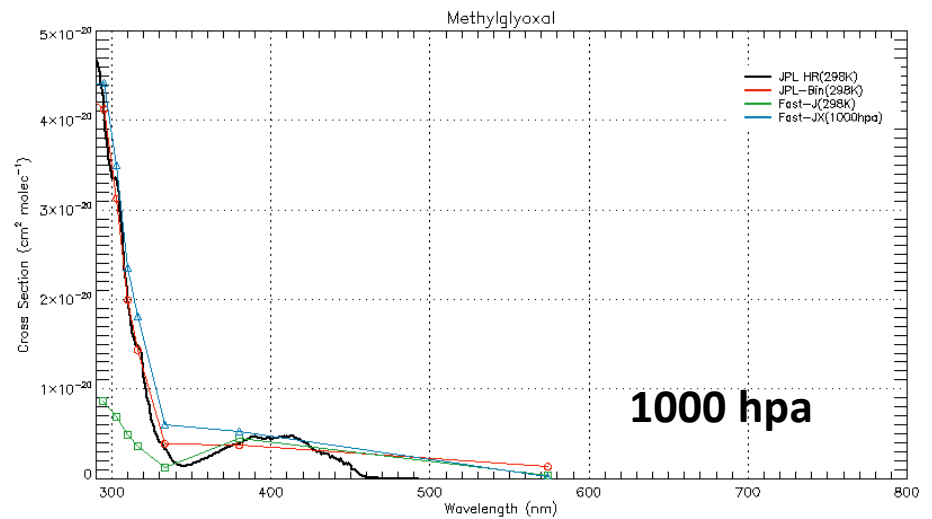
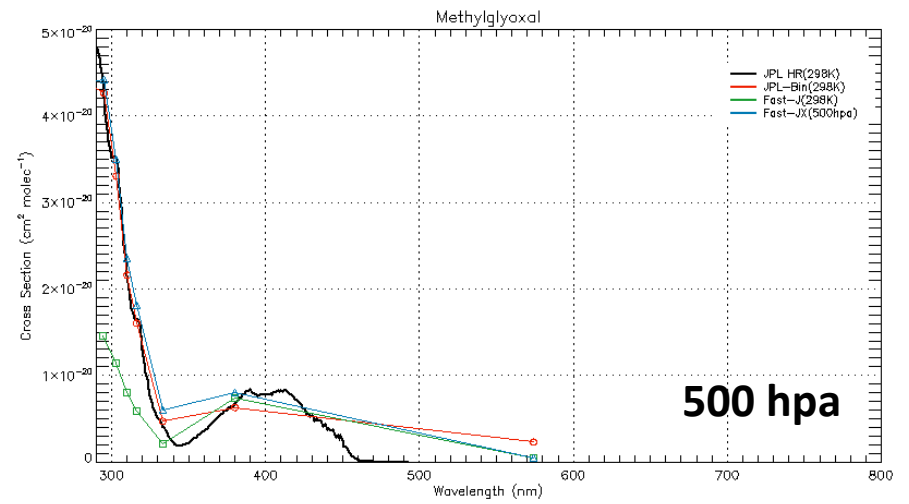
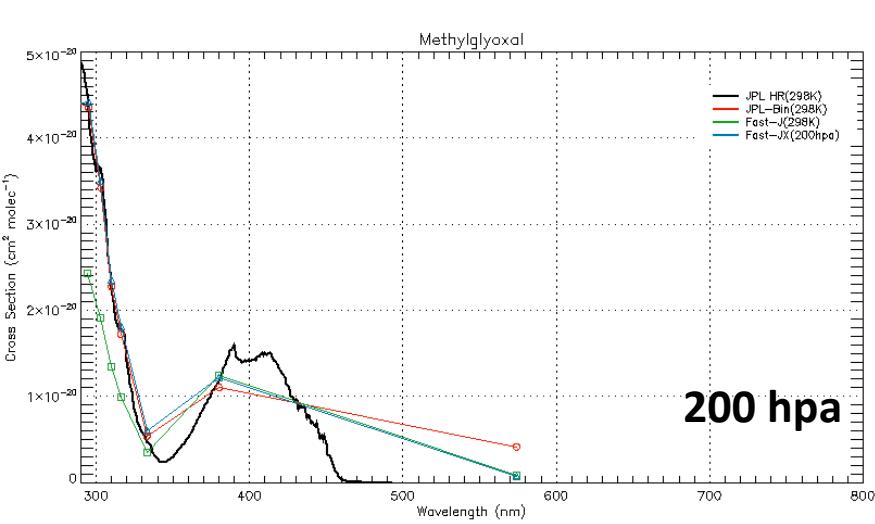
where $\Phi_0(\lambda) = (3.63 \pm 0.32) 10^{-7} [\exp(5693 \pm 533) / \lambda]$
and $k_0(\lambda) = (1.93 \pm 0.24) \times 10^8 [\exp(-5639 \pm 497) / \lambda]$

The zero pressure quantum yields, $\Phi_0(\lambda)$, are in good agreement for wavelengths ≤ 420 nm. However, the quantum yields at 760 Torr from the Chen et al. [42] and Koch and Moortgat [97] expressions deviate by a 4D-41

Applies to: MGLY

factor 4 for wavelengths ≥ 420 nm. The data from the more direct study by Chen et al. [42] are recommended. Additional measurements are needed to establish the quantum yields in the long wavelength tail of the spectrum at atmospheric relevant pressures.

D23 - MGLY



IUPAC - MEK

Primary photochemical transitions

Reaction		$\Delta H_{298}^{\circ}/\text{kJ}\cdot\text{mol}^{-1}$	$\lambda_{\text{threshold}}/\text{nm}$
$\text{CH}_3\text{C}(\text{O})\text{C}_2\text{H}_5 + h\nu$	$\rightarrow \text{CH}_3 + \text{C}_2\text{H}_5\text{CO}$ (1)	352.6	339
	$\rightarrow \text{C}_2\text{H}_5 + \text{CH}_3\text{CO}$ (2)	349.4	342
	$\rightarrow \text{CH}_3 + \text{C}_2\text{H}_5 + \text{CO}$ (3)	395.3	

Absorption cross-section data

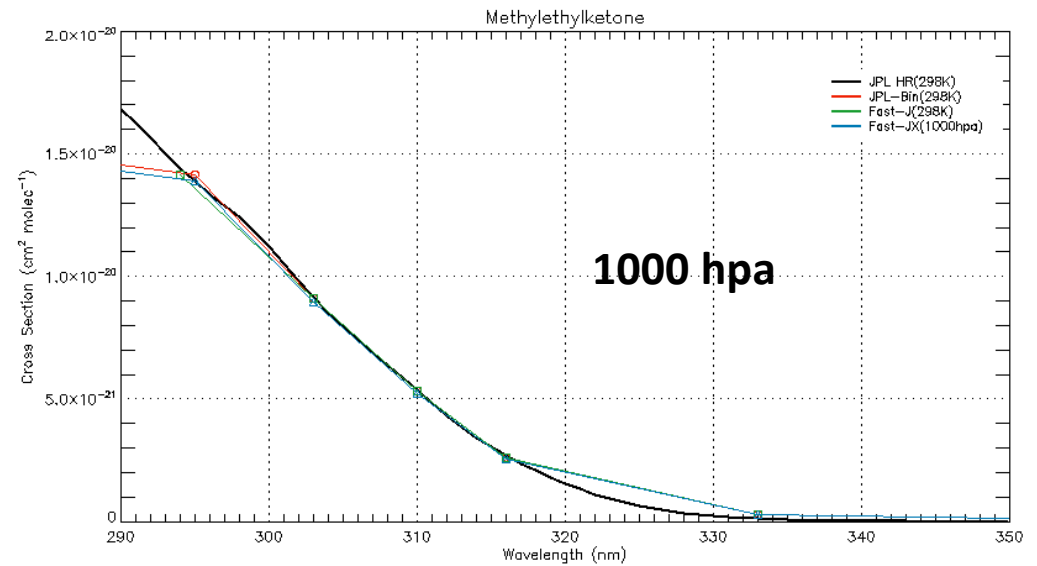
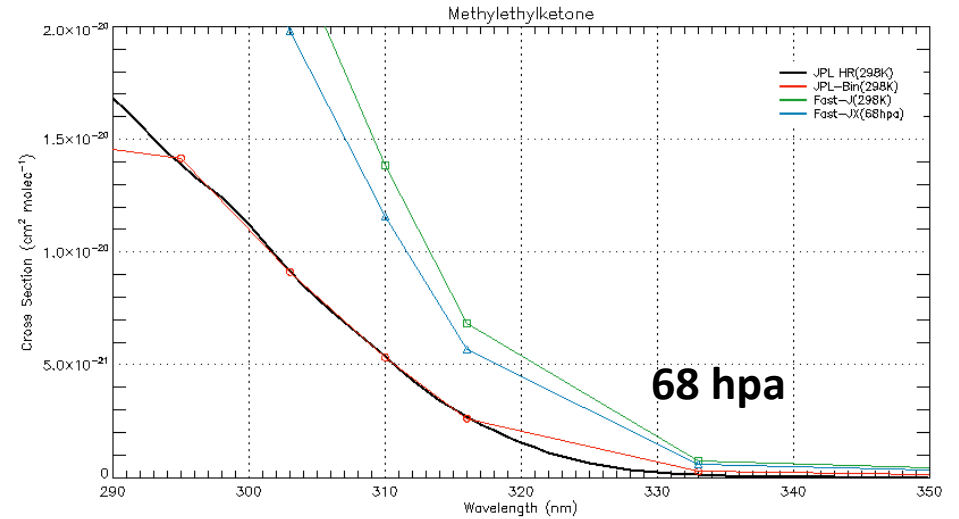
Wavelength range/nm	Reference	Comments
202–355	Martinez et al., 1992	(a)
240–350	Yujing and Mellouki, 2000	(b)

Quantum yield data ($\phi = \phi_1 + \phi_2 + \phi_3$)

Measurement	Wavelength range/nm	Reference	Comments
ϕ_1 0.34 (1000 mbar) 0.89 (68 mbar)	275–380	Raber and Moortgat, 1987	(c)

Applies to: MEK

IUPAC - MEK



IUPAC – ONIT1

Primary photochemical transitions

Reaction		$\Delta H_{298}^{\circ}/\text{kJ}\cdot\text{mol}^{-1}$	$\lambda_{\text{threshold}}/\text{nm}$
$n\text{-C}_3\text{H}_7\text{ONO}_2 + h\nu$	$\rightarrow n\text{-C}_3\text{H}_7\text{O} + \text{NO}_2$	(1) 165.9	721
	$\rightarrow \text{C}_2\text{H}_5\text{CHO} + \text{HONO}$	(2) -92.8	
	$\rightarrow \text{C}_3\text{H}_7\text{ONO} + \text{O}(\text{^3P})$	(3)	

Absorption cross-section data

Wavelength range/nm	Reference	Comments
270–330	Roberts and Fajer, 1989	(a)
185–330	Turberg et al., 1990	(b)
220–340	Clemmitshaw et al., 1997	(c)

Comments

- Absorption cross-sections were measured in a cell of 10.2 cm pathlength using a single-beam spectrometer with a photometric accuracy of $\pm 0.5\%$. No NO_2 could be detected by FTIR in the n -propyl nitrate.
- Absorption cross-sections were measured in 2 cm and 10 cm pathlength cells with a range of pressures of $n\text{-C}_3\text{H}_7\text{ONO}_2$ at an unspecified spectral resolution.
- Absorption cross-sections were measured with a dual-beam diode array spectrometer, with a spectral resolution of approximately 0.6 nm. The purity of the n -propyl nitrate was checked by NMR and FTIR.

Comments on Preferred Values

Clemmitshaw et al. (1997) have measured the absorption cross-sections at 298 K over the range 220 nm to 340 nm. In the wavelength region where their measurements overlap with those of Roberts and Fajer (1989) (270 nm to 320 nm), the two studies are in excellent agreement. Agreement with the results of Turberg et al. (1990) is also very good in the range 220 nm to 295 nm, but the results of Turberg et al. (1990) deviate significantly from those of both Clemmitshaw et al. (1997) and Roberts and Fajer (1989) at $\lambda > 295$ nm. This tendency to obtain higher values than others of the absorption cross-section at longer wavelengths is noticeable in the results of Turberg et al. (1990) in all of their studies of the higher nitrates and could be due to traces of NO_2 in their samples.

The preferred values of the absorption cross-section are those of Turberg et al. (1990) for the range 185 nm to 220 nm where theirs are the only measurements. Over the range 220 nm to 295 nm averages are taken of the results of Roberts and Fajer (1989), Turberg et al. (1990) and Clemmitshaw et al. (1997) where their studies overlap, and over the range 295 nm to 340 nm the preferred values are based on the results of Roberts and Fajer (1989) and Clemmitshaw et al. (1997).

There are no data on either the products of photodissociation or the quantum yields. However, the quantum yields for photodissociation of both ethyl and methyl nitrate to form NO_2 have been shown to be unity at 308 nm and 248 nm, respectively (see data sheets in this evaluation). Since the absorption spectra of organic nitrates are very similar, with structureless continua occurring in the same region of the spectrum, it seems likely that the photodissociation quantum yield for n -propyl nitrate will also be unity. Further support for this conclusion comes from direct measurements (Luke et al., 1989) of the rate of formation of NO_2 from the photolyses of $n\text{-C}_3\text{H}_7\text{ONO}_2$ in sunlight. These agreed well with the calculated rates of photolyses, based on measurements of the absorption cross-sections, solar irradiances, and an assumed value of $\phi_1=1$ throughout the wavelength region 290 nm to 340 nm (Luke et al., 1989).

**Applies to: MACRN, MVKN, ISOPNB,
ISOPND, PROPNN**

IUPAC – ONIT1

